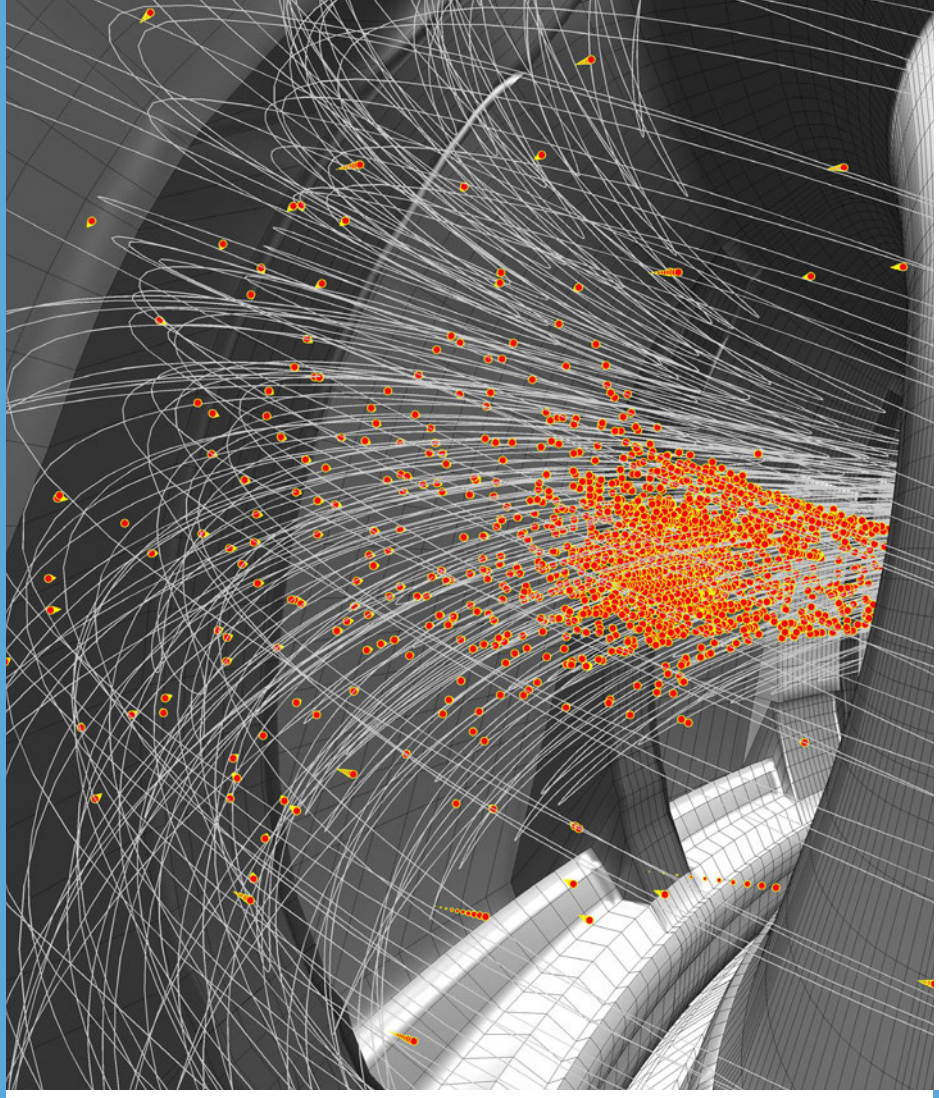

SCIENCE • TECHNOLOGY • RESEARCH HIGHLIGHTS • VISIONS •

Dissertation
10

Fast ions and momentum transport in JET tokamak plasmas

Antti Salmi

VTT

VTT SCIENCE 10

Fast ions and momentum transport in JET tokamak plasmas

Antti Salmi
VTT, Espoo

Thesis for the degree of Doctor of Science (Tech.) to be presented with due permission of the School of Science for public examination and criticism in Auditorium E, at the Aalto University School of Science (Espoo, Finland) on the 9th of November 2012 at 12 noon.

ISBN 978-951-38-7467-4 (soft back edition)
ISSN 2242-119X (soft back edition)

ISBN 978-951-38-7468-1 (http://www.vtt.fi/publications/index.jsp)
ISSN 2242-1203 (http://www.vtt.fi/publications/index.jsp)

JULKAISIJA - UTGIVARE - PUBLISHER

VTT
PL 1000 (Tekniikantie 4 A, Espoo)
02044 VTT
Puh. 020 722 111, faksi 020 722 7001

VTT
PB 1000 (Teknikvägen 4 A, Esbo)
FI-02044 VTT
Tfn. +358 20 722 111, telefax +358 20 722 7001

VTT Technical Research Centre of Finland
P.O. Box 1000 (Tekniikantie 4 A, Espoo)
FI-02044 VTT, Finland
Tel. +358 20 722 111, fax + 358 20 722 7001

Kopijyvä Oy, Kuopio 2012

Fast ions and momentum transport in JET tokamak plasmas

Antti Salmi. Espoo 2012. VTT Science 10. 71 p. + app. 75 p.

Abstract

Fast ions are an inseparable part of fusion plasmas. They can be generated using electromagnetic waves or injected into plasmas as neutrals to heat the bulk plasma and to drive toroidal rotation and current. In future power plants fusion born fast ions deliver the main heating into the plasma. Understanding and controlling the fast ions is of crucial importance for the operation of a power plant. Furthermore, fast ions provide ways to probe the properties of the thermal plasma and get insight of its confinement properties.

In this thesis, numerical code packages are used and developed to simulate JET experiments for a range of physics issues related to fast ions. Namely, the clamping fast ion distribution at high energies with RF heating, fast ion ripple torque generation and the toroidal momentum transport properties using NBI modulation technique are investigated.

Through a comparison of numerical simulations and the JET experimental data it is shown that the finite Larmor radius effects in ion cyclotron resonance heating are important and that they can prevent fast ion tail formation beyond certain energy. The identified mechanism could be used for tailoring the fast ion distribution in future experiments. Secondly, ASCOT simulations of NBI ions in a ripple field showed that most of the reduction of the toroidal rotation that has been observed in the JET enhanced ripple experiments could be attributed to fast ion ripple torque. Finally, fast ion torque calculations together with momentum transport analysis have led to the conclusion that momentum transport in not purely diffusive but that a convective component, which increases monotonically in radius, exists in a wide range of JET plasmas. Using parameter scans, the convective transport has been shown to be insensitive to collisionality and q-profile but to increase strongly against density gradient.

Keywords: JET, tokamak, fusion, energy, plasma, toroidal rotation, momentum transport, fast ions, neutral beam injection, NBI

Nopeat ionit ja liikemäärän kulkeutuminen JET-tokamakin plasmoissa

Antti Salmi. Espoo 2012. VTT Science 10. 71 s. + liitt. 75 s.

Tiivistelmä

Nopeat ionit ovat erottamaton osa fuusioplasmoja. Niitä voidaan tuottaa sähkömagneettisten aaltojen avulla tai suihkuttamalla ne plasmaan energisinä neutraaleina. Nopeita ioneja käytetään kuumentamaan ja pyörittämään plasmaa, virranajossa sekä plasman ominaisuuksien ja koossapidon tutkimiseen. Tulevaisuuden voimalaitoksissa fuusioreaktioissa syntyvät nopeat ionit toimivat plasman pääasiallisena lämmönlähteenä. Nopeiden ionien ilmiöiden ymmärtäminen ja niiden hallinta ovat tärkeitä fuusiovoimaloiden operoinnin kannalta.

Tässä väitöstyössä käytetään ja kehitetään numeerisia laskentaohjelmia selittämään nopeisiin ioneihin liittyviä koetuloksia Englannissa sijaitsevassa fuusiokoelaitoksessa (JET). Tutkimuksen kohteina ovat nopeiden ionien äkillinen väheneminen korkeilla energioilla radiotaajuuskuumennuksen yhteydessä, nopeiden ionien aiheuttama toroidaalinen vääntö magneettikentän ryppyisyyden vaikutuksesta ja liikemäärän kulkeutumisen ominaisuudet moduloituja neutraalisuihkuja käyttäen.

Työssä todennettiin simuloinneilla, että ionien äärellinen pyörimissäde selittää kokeellisesti havaitun nopeiden ionien pienen lukumäärän korkeilla energioilla käytettäessä radiotaajuuskuumennusta. JET:n magneettikentän rypytyskokeissa havaitut plasman pyörimisen muutokset voitiin hiukkassimulointien avulla päätellä johtuvan pääasiassa nopeiden ionien synnyttämän väännön takia. Lopulta analyysit liikemäärän kulkeutumisesta useissa erilaisissa plasmoissa osoittivat, että liikemäärän kulkeutuminen ei ole pelkästään diffuusia ja että merkittäväksi osoittautunut koossapitoa parantava ajautumisnopeus kasvaa plasman ulkoreunaa lähestyttäessä. Plasman tiheysgradientin kasvattamisen havaittiin nopeasti kasvattavan ajautumisnopeutta, kun taas törmäyksellisyyden tai q-profiilin muutosten vaikutukset olivat pieniä. Työn tuloksia voidaan hyödyntää ITERin ja tulevien laitosten suunnittelussa ja plasman pyörimisen ennustuksissa.

Keywords: JET, tokamak, fusion, energy, plasma, toroidal rotation, momentum transport, fast ions, neutral beam injection, NBI

Preface

The research summarized in this thesis has been carried out partially at the Aalto University, partially at the Joint European Torus (JET), Abingdon, UK and partially at the VTT Technical Research Centre of Finland. Several people have given important contributions to make this thesis possible and to whom I'm deeply grateful. First of all, I wish to thank Rainer Salomaa for granting me a PhD position in fusion and for his advise along the way. I'm also in debt to Seppo Karttunen for pulling the strings and for his encouragement when sending me for two long term secondments to JET.

Over the past years at the Aalto University, JET and VTT I've had the pleasure to work with many brilliant scientists from whom I've learned a great deal. My group leader at JET, Vassili Parail, always had new ideas for research and was continuously willing to help when I needed physics insights or got stuck on something. Mervi Mantsinen, Thomas Johnson and Tuomas Tala have all had important roles by sharing their vast knowledge on several areas of plasma physics and in teaching me the art of research.

The discussions during lunch and coffee breaks, and over pints, with Martin Laxåback, Marko Santala and Johnny Lönnroth have been an invaluable source of inspiration and deserve a special mention. I also thank Otto Asunta and Seppo Sipilä for their help with the ASCOT code.

Finally, the biggest thanks of all belongs to my parents and siblings, and to my family Anna, Eero and Emma for their love, support and understanding.

The financial support from Fortum Säätiö and Väisälän rahasto are gratefully acknowledged.

Espoo, October 17, 2012,

Antti Salmi

Academic dissertation

Supervisor	Professor Rainer Salomaa Department of Applied Physics Aalto University School of Science, Finland
Instructor	Dr Tuomas Tala Fusion and Plasma Technology VTT Technical Research Centre of Finland
Reviewers	Professor Torbjörn Hellsten Fusion Plasma Physics KTH Royal Institute of Technology, Sweden
	Dr Giovanni Tardini Institut für Plasmaphysik Max Planck Institut, Germany
Opponent	Dr Clarisse Bourdelle Institute of Magnetic Fusion Research CEA Cadarache, France

Contents

List of publications

This thesis consists of an overview and of the following publications which are referred to in the text by their Roman numerals.

I A. Salmi, M.J. Mantsinen, P. Beaumont, P.C. de Vries, L-G Eriksson, C. Gowers, P. Helander, M. Laxåback, J-M Noterdaeme, D. Testa and EFDA JET contributors. JET experiments to assess the clamping of the fast ion energy distribution during ICRF heating due to finite Larmor radius effects. *Plasma Physics and Controlled Fusion*, **48**, 717–726, 2006.

II A. Salmi, T. Johnson, V. Parail, J. Heikkinen, V. Hynönen, T.P. Kiviniemi, T. Kurki-Suonio and JET EFDA Contributors. ASCOT Modelling of Ripple Effects on Toroidal Torque. *Contributions to Plasma Physics*, **48**, 77–81, 2008.

III P.C. de Vries, A. Salmi, V. Parail, C. Giroud, Y. Andrew, T.M. Biewer, K.Crombé, I. Jenkins, T. Johnson, V. Kiptily, A. Loarte, J. Lönnroth, A. Meigs, N. Oyama, R. Sartori, G. Saibene, H. Urano, K.-D. Zastrow and JET EFDA Contributors. Effect of toroidal field ripple on plasma rotation in JET. *Nuclear Fusion*, **48**, 035007 (6pp), 2008.

IV P.C. de Vries, T.W. Versloot, A. Salmi, M-D Hua, D.H. Howell, C. Giroud, V. Parail, G. Saibene, T. Tala and JET EFDA Contributors. Momentum transport studies in JET H-mode discharges with an enhanced toroidal field ripple. *Plasma Physics and Controlled Fusion*, **52**, 065004 (11pp), 2010.

V A. Salmi, T. Tala, G. Corrigan, C. Giroud, J. Ferreira, J. Lönnroth, P. Mantica, V. Parail, M. Tsalas, T.W. Versloot, P.C. de Vries, K.-D. Zastrow and EFDA JET Contributors. NBI torque in the presence of magnetic field ripple: experiments and modelling for JET. *Plasma Physics and Controlled Fusion*, **53**, 085005 (20pp), 2011.

VI T. Tala, A. Salmi, C. Angioni, F.J. Casson, G. Corrigan, J. Ferreira, C. Giroud, P. Mantica, V. Naulin, A.G. Peeters, W. Solomon, D. Strintzi, M. Tsalas, T.W. Versloot, P.C. de Vries, K.-D. Zastrow and JET EFDA Contributors. Parametric dependences of momentum pinch and Prandtl number in JET. *Nuclear Fusion*, **51**, 123002 (11pp), 2011.

Author's contribution

Publication I: "JET experiments to assess the clamping of the fast ion energy distribution during ICRF heating due to finite Larmor radius effects"

The author used the combination of Fokker-Planck code PION and bounce averaged Monte Carlo code FIDO for calculating the fast hydrogen distribution during 2^{nd} harmonic ICRF heating. The agreement with experimental NPA measurements confirmed that FLR effects are important and responsible for the lack of multi-MeV ions during the 2^{nd} harmonic heating. The author wrote the full paper.

Publication II: "ASCOT Modelling of Ripple Effects on Toroidal Torque"

The author improved ASCOT code in order to record and calculate the total torque from the JET NBI system. The author made all the simulations which showed that ripple reduces the torque from JET NBI much more effectively than what it does for power losses. The author wrote the full paper.

Publication III: "Effect of toroidal field ripple on plasma rotation in JET"

The functionality developed in Publication II was utilised in this work to analyse a series of JET discharges with varying level of ripple. The author made all the NBI torque calculations and related data analysis and contributed to understanding the results. Figures 4 and 5 include ASCOT data and show the importance of the

fast ion ripple torque in explaining the observed toroidal rotation. The author also contributed in the parts of the text with ASCOT data and description.

Publication IV: "Momentum transport studies in JET H-mode discharges with an enhanced toroidal field ripple"

ASCOT calculations of NBI torque were used here to gain insight on the momentum transport properties of the JET plasmas. By taking into account the reduction in the NBI torque due to ripple it was possible to isolate the effect of transport and sources and deduce the average level diffusive and convective transport over a number of NBI heated JET discharges. The author contributed to this analysis by making NBI torque calculations (Figures 1 and 2) and in writing ASCOT related parts of the manuscript.

Publication V: "NBI torque in the presence of magnetic field ripple: experiments and modelling for JET"

The author extended ASCOT code functionality for time dependent operation and utilised it to obtain realistic time dependent NBI torque to analyse the experimental data. Furthermore, the author developed an optimisation framework around JETTO transport code to iteratively deduce the momentum transport properties of the discharges. These enabled the first experimental benchmark of calculated NBI torque in the presence of toroidal magnetic field ripple. The author wrote the full paper.

Publication VI: "Parametric dependences of momentum pinch and Prandtl number in JET"

In this work NBI is used as a tool to study the toroidal momentum transport properties of a number of plasmas to establish how it varies with q, collisionality and density gradient scale length. The author contributed through ASCOT torque analysis and transport analysis leveraging on techniques established in Publication V. These data are the basis for the results shown in sections 3 and 4.

1. Introduction

1.1 Fusion for energy

The ever increasing consumption of energy [1, 2] in the world together with environmental constraints demand the development of clean and sustainable forms of energy production. In the long term thermonuclear *fusion* could play a significant role in meeting these requirements. The fusion reaction providing the simplest route for fusion power production on Earth is between hydrogen isotopes deuterium and tritium

$$ {}^{2}_{1}\mathrm{D} + {}^{3}_{1}\mathrm{T} \rightarrow {}^{4}_{2}\mathrm{He}\ (3.52\ \mathrm{MeV}) + {}^{1}_{0}\mathrm{n}\ (14.1\ \mathrm{MeV}) \tag{1.1} $$

Deuterium can be extracted from water ($\sim$150 ppm) and tritium can be processed from lithium using neutrons from the fusion reactions within the fusion power plant itself

$$ {}^{6}_{3}\mathrm{Li} + {}^{1}_{0}\mathrm{n} \rightarrow {}^{4}_{2}\mathrm{He}\ (2.05\ \mathrm{MeV}) + {}^{3}_{1}\mathrm{T}\ (2.73\ \mathrm{MeV}) \tag{1.2} $$

The deuterium reserves last millions of years and the known lithium reserves for tens of thousands of years at the current level of consumption. The fuel for fusion is found all around the world making it geopolitically stable, fusion does not produce greenhouse gases or long lived radioactive waste and it has minimal impact on land use. Fusion power plants are ideally suited for large scale electricity production to provide a steady base load all year round.

In Europe the fusion research program is coordinated within the framework of the European Fusion Development Agreement (EFDA) which is funded by the European Commission. The current EFDA budget is roughly 100 million euros half

of which goes towards operating the largest tokamak to-date, the Joint European Torus (JET) in Abingdon, UK.

1.2 Tokamaks

Currently the most advanced concept for a fusion power plant in terms of fusion power is a *tokamak* which encloses the plasma inside a doughnut shaped chamber using strong toroidal magnetic field. The word *tokamak* is an acronym from the Russian words ***to****roidal'naya* ***kam****era s* ***ak****sial'nym magnitnym polem*, i.e. toroidal chamber with axial magnetic field. A simplified illustration of a tokamak, where the plasma is confined by a strong toroidal field in a doughnut shaped vessel with the plasma itself acting as the secondary winding, is shown in Fig. 1.1. The major benefit of this device the lack of ends in the tokamak 'bottle', made it significantly more efficient in confining the plasma while the primary transformer circuit allowed poloidal field generation and Ohmic heating via induction.

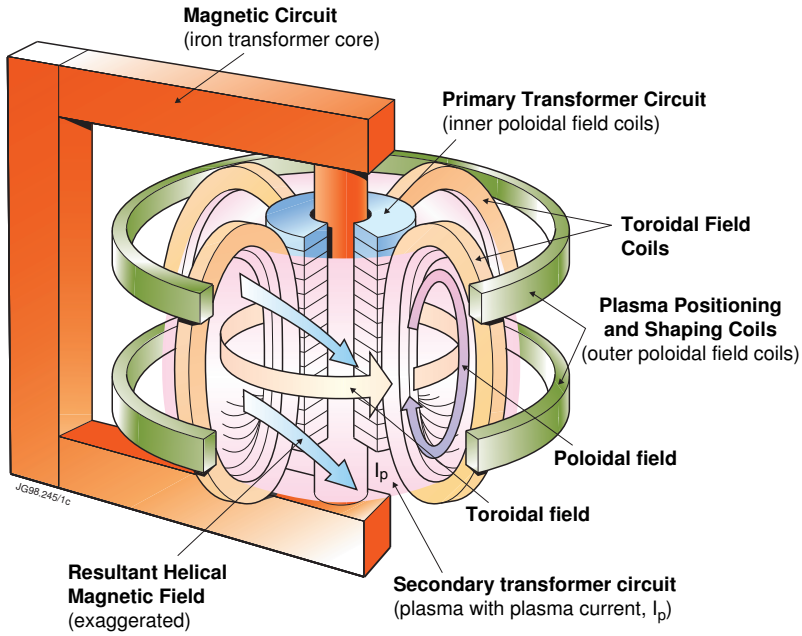

Figure 1.1. Tokamak principle. Ohmic heating and current drive is induced by the transformer where the plasma itself acts as the secondary winding. The iron core is optional when the primary winding is located along the toroidal axis inside the torus (central solenoid). *Courtesy of EFDA-JET.*

The tokamak was invented and first built during the cold war in the 1950s in Soviet Union [3]. It proved to be a superior concept outperforming the earlier devices (z-pinch, θ-pinch, etc.) in fusion power by orders of magnitude. Even though the first H-bombs were tested in 1952 in the USA and the cold war was still escalating between the super-powers, the magnetically confined fusion research was quickly declassified and researchers were encouraged to collaborate and find ways to harness the practically endless energy source for peaceful power production. The breakthrough raised hopes for a quick realisation of commercial power production. Indeed the following decades saw fusion power increase at a rate surpassing the famous Moore's Law in semiconductors.

As the tokamaks grew larger and more reactor relevant many new challenges were identified (instabilities, turbulence, materials) which together with increasing cost of building larger and larger devices and reduced funding due to the low cost of fossil fuels pushed the dream of commercial fusion power into the future. Presently the largest tokamak in the world, JET (Joint European Torus, see Fig. 1.2) in Oxfordshire, UK, has demonstrated 16 MW of peak fusion power and 4 MW in steady state conditions [4].

The next step experimental device being built in France, ITER [5–7], is a 15 billion euro international project involving over half of the world population (EU, US, Japan, Russia, China, India and Korea) and it is designed to be able to produce 500 MW of fusion power whilst using only 50 MW of external power to heat the plasma. If, and hopefully when, ITER proves to be a success the next step could be to build a demonstration power plant, DEMO, which would integrate all the technologies tested in ITER and those from the parallel materials research program into one plant for testing the power production. With successful integration of technologies and advances in fusion relevant materials, the era of fusion power could well begin on the second half of this century.

1.3 Heating and stabilising the plasma

In order to bring the plasma temperature up to the required 150 million degrees (10–20 keV) powerful plasma heating methods are needed. The Ohmic heating alone, generated by the induction, is not sufficient. It cannot heat up fusion plasmas beyond 4 keV due to the reduced resistivity of the plasma at high tempera-

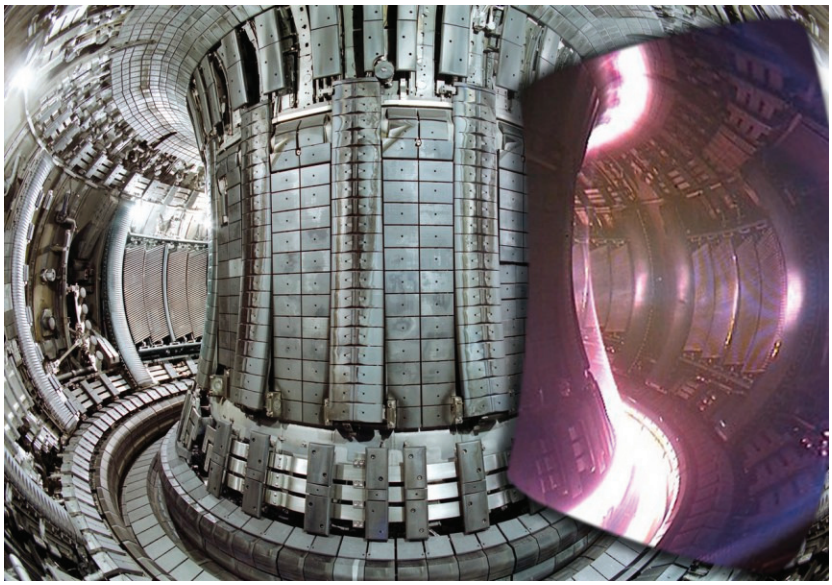

Figure 1.2. Wide angle view from inside the JET tokamak. On right, plasma discharge is overlaid. The white light during the plasma discharge indicates the high heat flux regions, the electromagnetic emissions from the central plasma are largely outside the visible spectrum. *Courtesy of EFDA-JET.*

tures, i.e. $\nu \propto T_e^{-3/2}$. Furthermore, Ohmic heating is intrinsically pulsed in nature which is not attractive from engineering point of view. In power plants the Ohmic heating would mainly be used for the start-up phase after which non-inductive means of heating and current drive would be used to control and stabilise the burning plasma.

Due to the strong magnetic field used in tokamaks external energy can only be injected into the system either as energetic neutral particles (neutral beam injection, NBI) or by launching electromagnetic waves whose the energy is transferred to the plasma typically via a resonance interaction. Depending on the frequency and wavelength power can be absorbed either on ions (Ion Cyclotron Resonance Frequency, $\sim$50 MHz) or on electrons (Electron Cyclotron Resonance Frequency, $\sim$100 GHz) or used to drive current (Lower Hybrid Current Drive, $\sim$4 GHz).

1.4 Toroidal coordinates

A convenient coordinate system for treating tokamak plasmas is illustrated in Fig. 1.3. The toroidal angle ϕ increases counter-clockwise when viewed from

above, z points upward and R outwards forming a right handed (R, ϕ, z) system. Flux coordinates (r, θ) describe the nested flux surfaces.

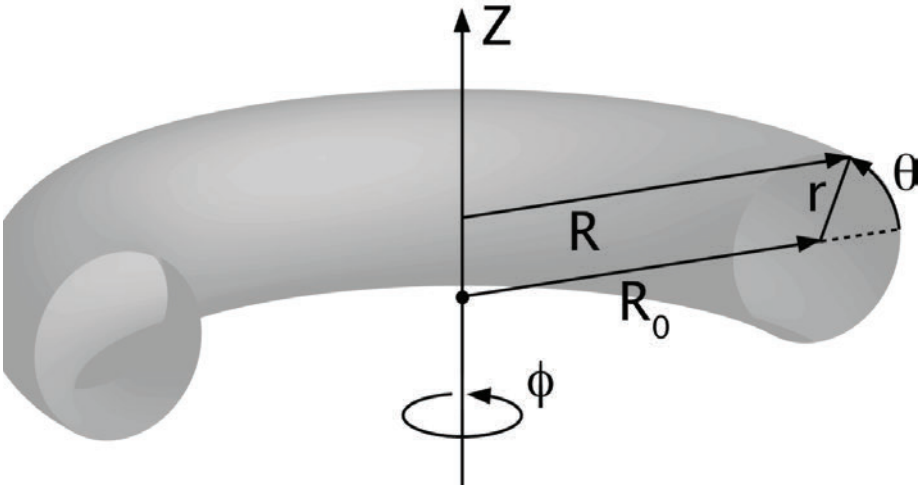

Figure 1.3. Simple toroidal coordinate system with circular flux surfaces.[1]

In most tokamaks flux surfaces are not circular and concentric as in this simplified picture but are elongated and radially shifted as given by the Grad-Shafranov equation [8] (see also Fig. 2.3). In these cases the geometrical coordinate r is not a convenient label any more and ρ_{tor} and ρ_{pol} are often used and appear in many of the figures plotted in this thesis and in Publications I–IV. Here ρ_{tor} is the normalised square root of the toroidal flux ψ_{tor} enclosed by the flux surface and ρ_{pol} is the correspondingly normalised label for the poloidal flux ψ_{pol} [8]. An important property of a flux surface is that by following a magnetic field line that starts from a certain flux surface always stays on that same surface. Since charged particles are tied to the field lines by Lorentz force (Sec. 2.1) they are also tied to the same flux surface and therefore, to a good approximation, plasma temperature and density are constant on a given flux surface. Ions and electrons can move freely along the field lines but only slowly across. This means that plasma confinement properties including heat and toroidal momentum transport can often be studied in radial direction only.

[1] http://www-fusion.ciemat.es/fusionwiki/index.php/Toroidal_coordinates

1.5 Outline of this thesis

This thesis in an introduction to and gives an overview of the main results obtained in the Publications I–VI. In Chapter 2 several relevant aspects of fast ion physics are briefly reviewed. First, motion of fast ions and their generation through ICRH (Publication I) and NBI (Publications II–VI) in the tokamak plasmas are described. Then the toroidal field ripple and its effect on fast ions is briefly reviewed together with a description of fast ion torque transfer to the background plasma. The last part of Chapter 2 gives an introduction to the toroidal momentum transport and NBI modulation technique which are used and studied in Publications V–VI. In Chapter 3 the simulation tools and methods are discussed together with a description of related modifications to them. Chapter 4 gives a short overview of the results obtained in Publications I–VI highlighting the most important findings. Finally the thesis is summarised.

2. Fast ion physics and transport

The definition of *fast* ion naturally depends on the context. In fusion plasmas fast ions are usually considered to be those whose kinetic energy exceeds the thermal energy of the bulk plasma by roughly a factor of 10. In today's medium to large sized tokamak devices the plasma temperature is typically in the range of 1-10 keV ($\sim$15 keV in future power plants) and therefore the lower energy limit for fast ions is somewhere around 10-100 keV, depending on a tokamak and a scenario. While in principle there is no upper limit for the fast ion energy in practice the size of the plasma and the strength of the magnetic field set constraints on the achievable fast ion energy. Namely, at high energies the orbits of the ions become so large that they are no longer confined in the plasma but collide with the torus walls. In JET, ions with energies up to 10 MeV have been observed. However, even the most energetic ions in fusion plasmas are far from the relativistic limit and their behaviour can be understood with classical treatment.

There are numerous reasons why fast ions are of interest to fusion plasmas. One of the most important one is their ability to transfer heat and momentum to the plasma. Fast ions interact with the ions and electrons of the main plasma via Coulomb collisions through which they transfer their energy and kinetic momentum. Toroidally asymmetric fast ion velocity distribution can drive current and induce toroidal plasma rotation. Fast ions can stabilise or destabilise some internal plasma instabilities such as sawteeth and enhance the fusion yield. On the other hand, fast ions can also have detrimental effects both on the plasma and the device. Namely, since the fast ions have large orbits and even a relatively small number of them can carry a significant fraction of the total plasma stored energy, their loss can damage the first wall, reduce the heating efficiency and modify the plasma rotation [9–12]. The free energy in the fast ions can in some

circumstances create instabilities (e.g. alfven eigenmodes) that reduce the plasma confinement. Understanding the creation and behaviour of the fast ion population in fusion plasmas is necessary to maximise their benefits and minimise their adverse effects.

2.1 Motion of charged particles

Compared to thermal ions, fast ion orbits are much wider and their distributions are often asymmetric and non-Maxwellian which means that their treatment is not usually realistic with fluid approach as often used for thermal plasma but that kinetic simulations are needed.

The motion of charged particles in an electromagnetic field is controlled by the Lorentz force

$$m\frac{d\mathbf{v}}{dt} = q(\mathbf{E} + \mathbf{v} \times \mathbf{B}) \tag{2.1}$$

Here, $\mathbf{E}$ and $\mathbf{B}$ are the electric and magnetic field vectors whereas m, q and $\mathbf{v}$ are the particle mass, charge and velocity, respectively. In absence of other interactions (e.g. collisions) particles can only gain energy through electric field which is parallel to the particle velocity (this is easily confirmed after taking the dot product of Eq. (2.1) with $\mathbf{v}$).

Due to the strong magnetic field used in tokamaks the gyro radius (or Larmor radius) $\rho = v_\perp/\omega_{ci}$ of a particle, where $v_\perp$ is the velocity perpendicular to the magnetic field and $\Omega_{ci} = qB/m$ is the gyro (or cyclotron) frequency, is often small compared to the typical scale lengths in the plasma. Furthermore, the time scales of interest are often much longer than the gyration period. In this case it is useful to average out the gyration and follow the guiding centre motion of the particle rather than its actual position. The averaging results in an equation for guiding centre motion [13]

$$\mathbf{v}_g = v_\parallel \hat{\mathbf{e}}_\parallel + \frac{\mathbf{F} \times \mathbf{B}}{qB^2} \tag{2.2}$$

$$\dot{v}_g = F_\parallel/m. \tag{2.3}$$

Here $\mathbf{F}$ is any force acting on the guiding centre such as electric field or non-uniformities in magnetic field. Figure 2.1 illustrates a typical orbit for an energetic, poloidally trapped, ion in a tokamak magnetic field. Just by glancing at

the trajectory it is easy to be convinced that in a realistic geometry where the magnetic field itself cannot be represented by simple equation the guiding centre equations are not analytically integrable and numerical codes are needed to trace the particles.

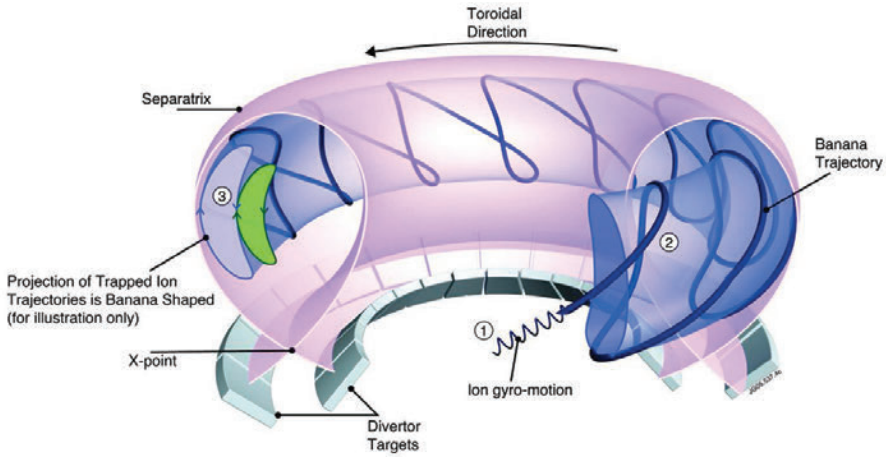

Figure 2.1. Trajectory of an energetic trapped ion in a tokamak equilibrium. (1) the gyration of the ion around the field line is shown with a thin line. (2) The thick line shows the guiding centre (gyro-averaged) motion of the ion. At (3) the poloidal cross section of the 3D trajectory is depicted. The smaller "banana" next to (3) illustrates the orbit of another ion that was launched, from the location where the two bananas are joined, in the opposite direction to the ion forming the larger banana. *Courtesy of EFDA-JET*

2.1.1 Constants of motion and adiabatic invariants

With stationary or slowly varying electromagnetic fields with toroidal symmetry charged particles have three invariants. Without collisions or other interactions they remain practically constant along the particle trajectory. These invariants can be chosen as the total energy E_{tot}, magnetic moment μ and the canonical toroidal angular momentum p_ϕ

$$E_{tot} = mv^2/2 + Ze\Phi \tag{2.4}$$

$$\mu = mv_\perp^2/2B \tag{2.5}$$

$$p_\phi = Ze\psi - mRv_\phi \tag{2.6}$$

where $\psi = \int_0^r RB_\theta dr'$ is the poloidal flux, Φ is the electrostatic potential, $v_\perp$ is the velocity perpendicular to the magnetic field, v_ϕ is the toroidal velocity, Z is the charge number and e is the elementary charge. Without toroidal symmetry the canonical toroidal angular momentum p_ϕ is no longer conserved. In non-axisymmetric magnetic field the radial transport of the charged particles is enhanced reducing the confinement and acts as a source for counter current torque (see Secs. 2.3 and 2.4).

2.2 Generation of fast ions

There are several ways to generate fast ions. Firstly, they are produced within the plasma in a number of different fusion reactions the most significant of which is the D-T fusion yielding a neutron and a 3.5 MeV alpha particle. In ITER, alphas will provide most of the plasma heating and are by far the most important fast ion species in the plasma. Of the current tokamaks only JET can operate D-T plasmas, and when it does it is a special event (tritium is expensive and difficult to handle due to its activity). Most of the time either deuterium or hydrogen plasmas are used and the fusion yields are too small to be of significance, apart from diagnostics purposes [14–16]. Therefore, the main source of fast ions in current devices comes either from neutral beam injection or through ion cyclotron resonance heating. In burning plasmas where alphas dominate the NBI and/or ICRH generated ions will still have an important role in driving current and rotation and in controlling the plasma

2.2.1 Neutral beam injection

Neutral beam injection (NBI) is a widely used method to non-inductively heat and drive current and rotation in the tokamak plasmas. NBI is a robust heating scheme which in current experiments can be used for nearly all plasmas without coupling issues or upper density limits. NBI also provides the most efficient way for inducing plasma rotation in current tokamaks. This is an important property of NBI since the plasma rotation and the rotation shear are known, experimentally and in theory, to improve plasma performance by clamping down the turbulence and the associated radial transport of heat, particles and momentum [17–19]. The reduced level of turbulence allows higher plasma temperature and

density thus improving the fusion yield and therefore potentially reducing the cost of the energy. Toroidal rotation is also known to stabilize magneto-hydodynamic (MHD) instabilities such as resistive wall modes (RWM) [20]. NBI generated torque and its usage to study rotation and momentum transport are discussed in more detail in Chapter 4.

The NBI system at JET [21] can deliver more than 20 MW of heating power and more than 20 Nm of torque routinely into the plasma. It consists of two beam boxes located toroidally 180 degrees apart, one in octant 4 and one in octant 8 (see Fig. 2.2). Both beam boxes consist of 8 positive ion neutral injectors (PINIs) of which 4 are in the so called tangential orientation and 4 in perpendicular orientation with respect to the toroidal magnetic field. In normal JET operation the plasma current is in the clockwise direction as indicated in the figure and the torque provided by the NBI is in co-current direction.

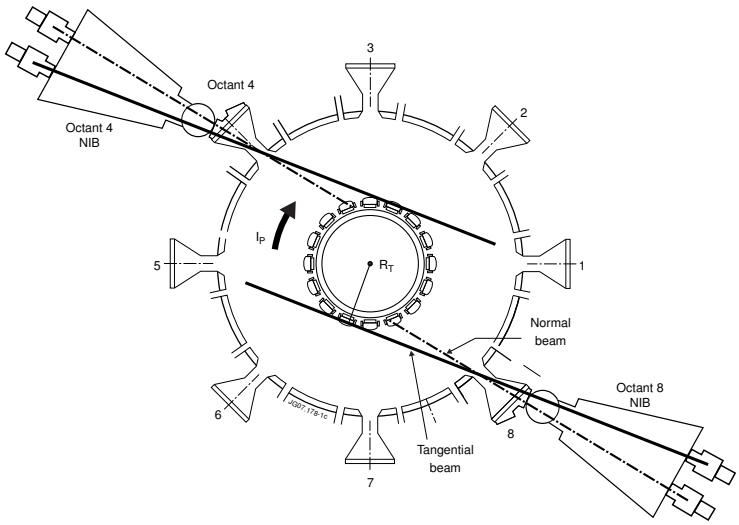

Figure 2.2. JET NBI system view from above (from Publication V).

The geometrical properties of the NBI system are fixed and the alignment cannot be changed during operation. Therefore the beams always point in the same direction in each experimental campaign. Figure 2.3 shows the poloidal alignment of each PINI in octant 8 NBI (octant 4 alignment is nearly identical). Reasonable flexibility to control the NBI heating and torque input is still retained as the PINI mixture, acceleration voltage of the PINIs and the power waveforms can be adjusted. The neutral beam modulation capability is in fact utilised in Publications

V-VI to validate the beam torque calculation and to study the momentum transport properties of the plasmas.

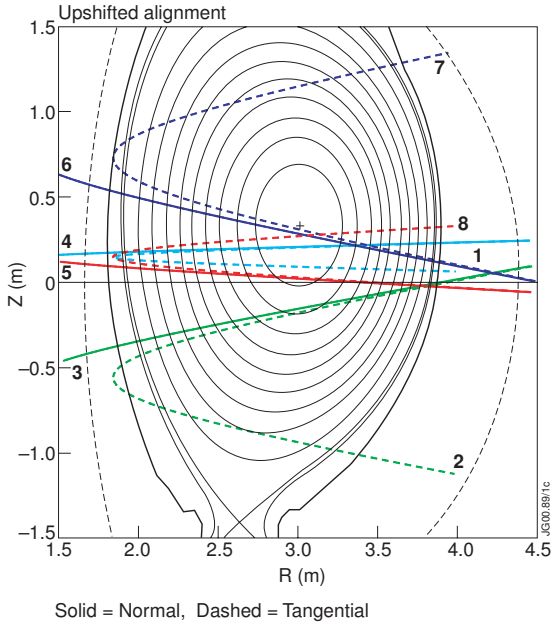

Figure 2.3. Poloidal view JET NBI alignment in the upshifted configuration. All beams enter the plasma near the midplane. The curvature of the trajectories results from 3D to 2D mapping. *Courtesy of EFDA-JET.*

The power from the neutral beams is absorbed in the plasma through Coulomb collisions. The heating rate (or the rate at which the beam loses energy) is given by

$$\frac{dE}{dt} = -(\nu_e + \sum_i \nu_i)E \tag{2.7}$$

where the summation loops over all ion species i in the plasma, E is the energy of the beam ion and ν_i, ν_e are the beam ion collision frequencies against the plasma ions and electrons, respectively. Substituting the collision frequencies this can be written as [13]

$$\frac{dE}{dt} = -\frac{Z^2 e^4 \ln\Lambda n_e}{4\pi\epsilon_0 m_e}\left[\frac{m_e}{n_e E^{3/2}}\sum_i \frac{n_i Z_i^2}{m_i} + \frac{4}{3\sqrt{\pi}}\left(\frac{m_e}{m k_B T_e}\right)^{3/2}\right]E \tag{2.8}$$

where in the usual circumstances the first term on the right hand side describes the heat deposition on the bulk ions and the second term the heat deposition on electrons. Here $\ln\Lambda \approx 17$ is the Coulomb logarithm, ϵ_0 is the permittivity of free

space, k_B is the Boltzmann constant, e is the elementary charge and m, Z, v are the mass, charge number and velocity respectively. Variables without subscripts refer to the beam ions. The collision frequency of the beam ions against electrons is independent of the beam ion energy ($\nu_e \sim n_e T_e^{-3/2}$) whereas against ions it becomes higher at low energy ($\nu_i \sim E^{-3/2}$). Therefore, at high energies the energetic ions interact mainly with electrons and at low with ions. The critical energy at which the ion and electron heating rates are equal is

$$E_{cr} = 14.8 k_B T_e A \left(\frac{1}{n_e} \sum_i \frac{n_i Z_i^2}{A_i} \right)^{2/3} \tag{2.9}$$

where A is the beam ion mass number and the summation loops over the background species. The quantity within the brackets varies slowly leaving the electron temperature and the beam ion mass as the only significant parameters that determine whether bulk ions or electrons are heated. In JET plasmas the critical energy is relatively high compared to the beam injection energy and the NBI is dominantly heating the ions. In ITER, however, beam injection energy of approximately 1 MeV is needed for deep enough penetration and therefore the NBI there will mainly heat the electrons.

2.2.2 Ion Cyclotron Resonance Heating

Ion Cyclotron Resonance Heating (ICRH) is the only heating method available for ITER that can dominantly heat ions [22]. The other common means of electromagnetically transmitting energy into the plasma, lower hybrid (LH) and electron cyclotron (EC) waves, are directly absorbed by the electrons. Furthermore, the collisional power transfer from both the alphas and the NBI ions result in dominant electron heating due to their high incident energy [23]. ICRH, however, can be optimised for ion heating by making sure that the average energy of the resonant ion population remains at reasonably low level. In ITER, the minority ^{3}He heating scheme is aimed for this and is expected to have an important role in setting the plasma conditions favourable for fusion reactions.

With ICRH scheme, radio frequency (RF) waves are launched with an antenna into the plasma where the power is absorbed by the resonating ions through wave-particle interaction (see Figs. 2.4 and 2.5).

Fusion plasmas can support a large number of electromagnetic waves with var-

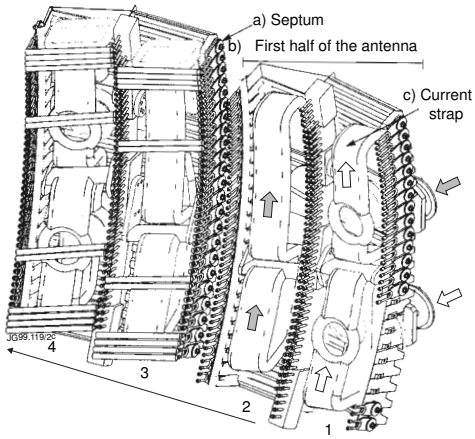

Figure 2.4. One of the four JET A2 antennas showing the first half of the antenna completely without the Faraday screens leaving the current straps visible. Thick arrows indicate that the AC current can be phased independently between the straps. Three A2 antennas, covered with Faraday screens, can be seen in Fig. 1.2. *Courtesy of EFDA-JET.*

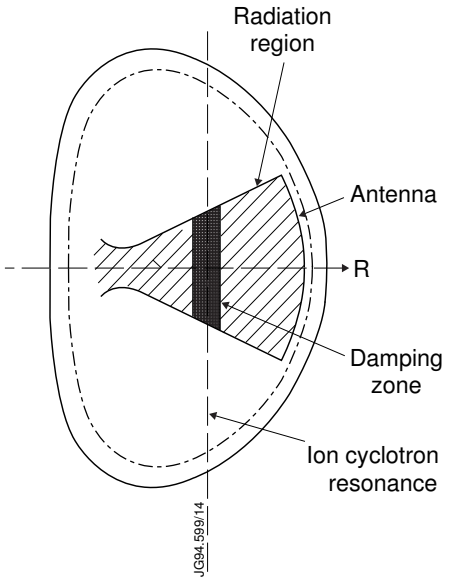

Figure 2.5. Schematic view of ICRF heating, wave propagation and damping in tokamak plasma. *Courtesy of EFDA-JET.*

ious frequencies and wave lengths. In ion cyclotron range of frequencies (20–80 MHz in fusion plasmas) the important branch in the plasma dispersion relation is the *fast wave* (or compressional hydromagnetic mode) [8, 24]. Fast wave does not exist in vacuum making it necessary to place the ICRH antenna relatively close to the plasma to avoid power being reflected back to the antenna. With close proximity to hot plasma, high heat fluxes must be tolerated and therefore the antennas are protected with heat bearing limiters.

Once the power reaches the plasma it can be absorbed. Provided that the frequency of the wave and the heating scheme are suitably selected most of the power will be absorbed by ions whose gyro-frequency or its harmonic equals the Doppler shifted wave frequency ($\nu = 0$)

$$\nu \equiv \omega - n\Omega_c - v_{\|}k_{\|} \tag{2.10}$$

where n is an integer, Ω_c is the gyro (or cyclotron) frequency of the ions, $v_{\|}$ is the ion velocity along the magnetic field line and $k_{\|}$ is the parallel wave number of the wave. In tokamaks the magnetic field is roughly proportional to 1/R which means that the gyro-frequency varies along the particle trajectories and that ions are resonant only for a short period when they cross the nearly vertical resonance layer. At the resonance position the ions see a constant electric field which can either accelerate or decelerate the ions depending on the relative phase between the wave and their gyration. When the relative phase between the successive RF interactions is random the quasi-linear theory states that this process is equal to diffusion in velocity space. In fusion relevant conditions the net effect is energy transfer from the waves to the particles.

Quasi-linear theory

According to quasi-linear theory [24, 25] the RF operator $Q(f)$ for a single wave can be written as a diffusion operator

$$Q(f) = \frac{1}{\partial v_{\perp}} \left(v_{\perp} D_{RF} \frac{\partial f}{\partial v_{\perp}} \right) \tag{2.11}$$

where the RF diffusion coefficient is proportional to

$$D_{RF} \sim \left| \tau_{RF} Ze(E_{+} J_{n-1}\left(k_{\perp}\rho\right) + E_{-} J_{n+1}(k_{\perp}\rho)) \right|^2 \tag{2.12}$$

where $E_{\pm}$ are the amplitudes of the left and right-hand polarized electric field components, $k_{\perp}$ is the local perpendicular wave number, J_m are the Bessel functions of the first kind and $\tau_{RF} = \int \exp(i \int \nu(t')dt')dt$ is the RF interaction time and n in an integer to indicate the resonance harmonic.

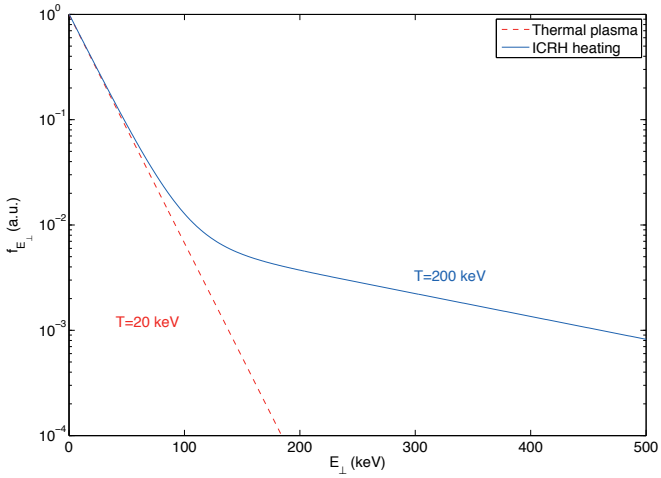

Figure 2.6. Schematic illustration of fast ion tail with strongly applied ICRF heating.

ICRH increases the perpendicular velocity of the resonating ions pulling a tail in the energy distribution as illustrated in the Fig. 2.6. The length of the tail and the effective temperature depend on the absorbed power per particle, fast ion collisionality (slowing down process) as well as other effects such as losses and instabilities [26]. The shape of the tail is usually more complex than in the idealised picture shown here. Realistic calculations of the fast ion distribution functions require the use of sophisticated codes such as PION and FIDO (see Chapter 3). In Publication I these tools are used to analyse JET experiments at the second harmonic ($n = 2$) ICRF heating that show the clamping of fast ion tail around the energy E^* where the first minimum of D_{RF} is located.

It is worth pointing out that while NBI is the most efficient method for driving toroidal rotation in current experiments also ICRH can modify the rotation profile somewhat either through momentum injection, fast ion losses or through transport modification [27–29]. A particular scheme where large rotation changes have been observed on Alcator-Cmod and JET involves mode conversion but is not yet fully understood [30, 31].

2.3 Toroidal field ripple

Toroidal magnetic field ripple (TF ripple) is the non-axisymmetric part of the magnetic field which arises due to the finite number of toroidal field coils. The ripple magnitude δ is defined as

$$\delta(R,z) = \frac{B_{\max}(R,z) - B_{\min}(R,z)}{B_{\max}(R,z) + B_{\min}(R,z)}, \tag{2.13}$$

i.e. it is the relative amplitude by which the magnetic field ripples (oscillates) when moving in toroidal direction (see Fig. 2.7).

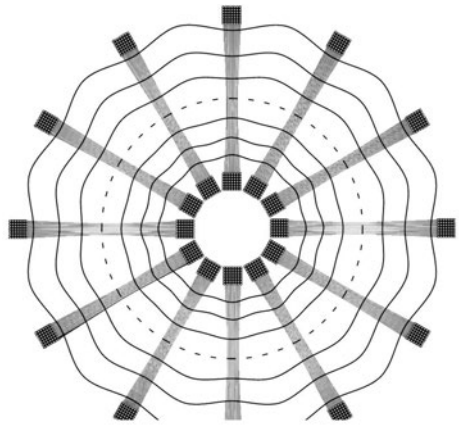

Figure 2.7. Toroidal field coils viewed from above. The toroidal field ripple arises due to the finite number of toroidal field coils. *Courtesy of EFDA-JET.*

TF ripple is an intrinsic property of all physical tokamaks. The magnitude of the ripple depends on the geometry and on the number of the coils and it is unique for each tokamak. Large levels of ripple have adverse effects on plasma confinement, especially on fast particle confinement [32, 33] and must be avoided. The ripple magnitude can be reduced by increasing the number of the coils and by making the coils larger. The downside of going this way is that the coils, especially if they are super-conducting, are typically the most expensive part of the device which together with the access requirements for maintenance, for diagnostics line-of-sights and for auxiliary heating systems means that some non-negligible level of ripple must always be tolerated.

Figure 2.8 shows the total magnetic field strength along a field line traced for one poloidal turn at $\rho_{pol} = 0.95$ for a JET discharge #77090. The large scale variation in the magnetic field is due to the $1/R$ dependence of the vacuum toroidal

field. The full line shows the total field with the exaggerated ripple included. The poloidal angle increases counter-clockwise and is zero at the outboard mid-plane. One can observe that ripple magnitude is largest at the LFS where it forms toroidally localised wells. In this region ripple effect is strongest and particles can get toroidally trapped due to the mirror force $F = -\mu\nabla_{\|}B$ [32].

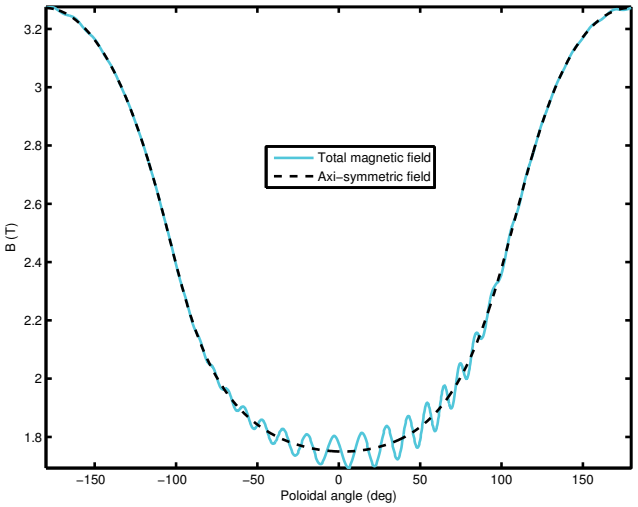

Figure 2.8. Total magnetic field strength for a JET discharge #77090 following a field line near separatrix for one poloidal turn. Dashed line shows the axi-symmetric contribution dominated by the 1/R dependence of the toroidal magnetic field and the full line shows the total strength including the ripple contribution (exaggerated).

In JET 32 toroidal field coils are used in normal operation. Uniquely among the current tokamak devices, JET can switch off every second coil or feed the even and odd numbered coils independently with different currents to adjust the level of ripple during experiments. Figure 2.9 depicts the numerical maps of the ripple magnitude δ for JET nominal operation with 32 coils and for the maximum possible ripple with every second coil turned off.

The shaded areas in the plasma show regions where ripple wells exist, i.e. regions where the gradient of the magnetic field strength along the magnetic field line changes sign due to the ripple (compare with Fig. 2.8). The existence of ripple wells depends also on the equilibrium magnetic field and is thus specific to each discharge. The boundary between ripple well region and region where ripple wells do not exist can be approximately described by the formula [34]

$$\alpha = \left| \frac{B_R}{BN\delta} \right| = 1 \tag{2.14}$$

where B_R is the major radius component of the equilibrium field and N is the number of toroidal field coils. Ripple wells exist for values $\alpha < 1$. The reason why ripple wells are of importance is because ions with small pitch $\xi = v_\parallel / v$ can be trapped toroidally. This can lead to rapid loss of ions due to the uncompensated vertical drift unless they de-trap either due to some interaction such as a collision or they pass through a region where ripple wells do not exist in which case they de-trap and remain in the plasma. For the JET plasmas studied here the ripple trapping for the NBI ions becomes important only at large ripple values $\delta > 1.5\%$.

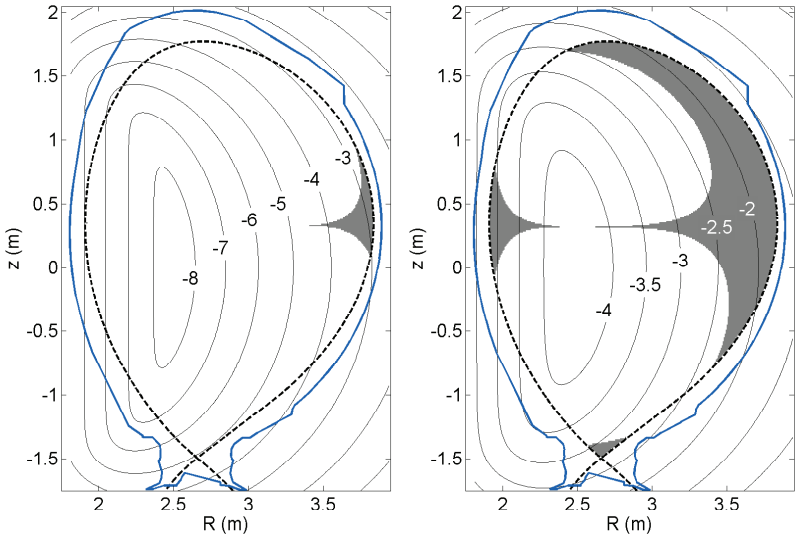

Figure 2.9. Toroidal magnetic field ripple δ plotted using $\log_{10}$ contours for a) the 32 coil operation and b) the 16 coil operation. Shaded areas show the regions where ripple wells exist (for plasmas similar to #77090).

Ripple magnitude varies strongly across the poloidal plane being largest on the outboard side close to the separatrix. Ripple decays exponentially in radius and becomes very small towards the core of the plasma. The decay length (away from the coils) for the 16 coil ripple magnitude is roughly 25 cm whereas it is half of that for the 32 coil case. When ripple magnitude is quoted it is customary to use a value which is either the maximum within the plasma or with respect to a fixed R-z coordinate. In the following the JET ripple magnitude is given at a location $R = 3.84$ m and $Z = 0$ m unless otherwise stated.

In general, the modelling capability of NBI sources for axi-symmetric plasmas

is considered to be good when neo-classical processes are dominating. However, prior to the work in this thesis the NBI torque sources in presence of toroidal field (TF) ripple were not well known despite the importance of ripple for ITER. In fact, the ASCOT calculations reported in Publication II are the first realistic fast ion ripple torque calculations in any tokamak.

2.3.1 Fast ions and ripple

Toroidal field ripple perturbs particle motion by giving rise to small oscillations in its velocity components and radial position

$$\tilde{v}_{\parallel} = -(v_{\perp}^2/2v_{\parallel})\delta \cos N\phi. \tag{2.15}$$

These oscillations are, however, self-cancelling along most of its trajectory. Significant contribution is only accumulated near the turning points of trapped particles where the oscillations are amplified ($v_{\parallel} \to 0$) and are not necessarily cancelled. For a simplified geometry the contribution around the turning point location can be integrated analytically using stationary phase method to yield a radial step size [35]

$$\Delta r = (N\pi/\theta_t)^{1/2}(q/\epsilon)^{3/2}\rho\delta \cos N\phi_t \tag{2.16}$$

where θ_t and ϕ_t are the poloidal and toroidal angles of the turning point location, q is the safety factor, ρ is the gyro radius and ϵ is the aspect ratio. It can be seen that the radial step size increases with particle energy $\Delta r \sim E^{1/2}$. Furthermore, since the diffusion coefficient scales like $D \sim (\Delta r)^2/\tau$ and the appropriate time scale (bounce time) is proportional to $\tau \sim E^{-1/2}$ the radial diffusion due to ripple depends strongly on energy $D \sim E^{3/2}$. Although very useful for physics insight the Eq. (2.16) is not accurate enough for quantitative calculations of fast ion ripple torque in an experiment. In this work ASCOT code is used to take into account ripple effects in realistic experimental geometry and in the presence of Coulomb collisions. All the intricacies of the ripple effect and the processes of trapping and de-trapping are trivially included in the guiding centre Monte Carlo approach where the ions are traced in the non-axisymmetric 3D magnetic field.

Theory has been developed for estimating the torque that results from the non-axisymmetric magnetic perturbations such as toroidal magnetic field ripple [36–40]. It has been applied to explain some experiments using resonant magnetic

perturbations (RMP) [41] but nevertheless it is rather sensitive to the collisionality regime and until so far it has not been shown to yield strong torques in the JET ripple field. Nevertheless, both in Tore Supra and in JET small negative rotation has been observed in Ohmic plasmas in the presence of large ripple [28, 42]. From the small counter current rotation in these discharges one can estimate that the magnitude of the Neoclassical Toroidal Viscosity (NTV) torque caused by the ripple should be quite modest. In this work the experimental observations and the modelling are indeed consistent with the assumption that NTV torque is small compared to the applied NBI torque. Finally, the supra-thermal electron losses ($\sim$200 keV) observed under strong LH heating in Tore Supra [43] are not expected to play a role in the typical JET plasmas with enhanced ripple where supra-thermal electrons are not present and therefore electron contribution to the torque is neglected.

2.4 Fast ion torque

Fast ions can transfer their toroidal momentum into the bulk plasma in two ways. First, simply via Coulomb collisions where part of fast ion toroidal kinetic momentum is absorbed by the bulk plasma $m\Delta v_\phi R$. The second mechanism ($j \times B$ – torque) for momentum transfer is somewhat less intuitive but in many cases of equal importance. It is associated with the radial current of fast ions [44] (see illustration in Fig. 2.10). Fast ion losses, fast ion ripple diffusion and injection of ions into trapped orbits are examples of processes which generate non-ambipolar fast ion currents. Due to the quasi-neutrality condition the plasma sets up a complex process to generate a *return* current that is equal but opposite to the fast ion current to cancel any charge accumulation. The torque on the plasma thus becomes

$$\tau_{j\times B} = j_{\mathrm{ret}} B_\theta R \tag{2.17}$$

where j_{ret} is the return current of the bulk plasma ($j_{\mathrm{ret}} = -j_{\mathrm{fast}}$), B_θ is the poloidal magnetic field and R is the major radius.

It is worth noting that while the radial return current also induces a poloidal torque it is usually not of interest because of the strong neoclassical damping of the poloidal flows [45–48]. On the other hand, toroidal direction in tokamaks is nearly symmetric which allows flows to develop. Therefore, in the following when

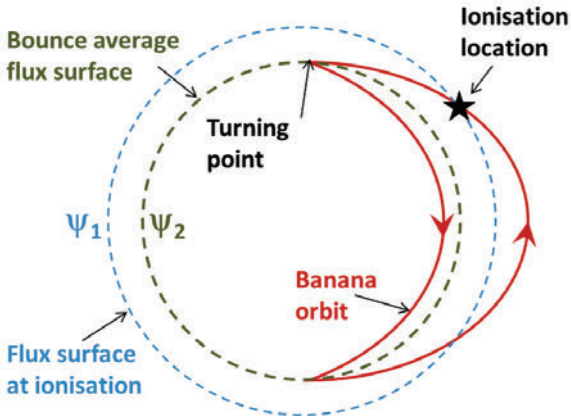

Figure 2.10. Schematic illustration of the instantaneous $j \times B$ – torque caused by the charge separation. Electron with thin orbit remains on the flux surface ψ_1 where the neutral is ionised while the trapped ion with a large orbit on average resides on its bounce averaged flux surface ψ_2. The torque on the plasma results from the radial return current that is set up to maintain quasi-neutrality.

torque is mentioned it is referring to the toroidal component of the torque.

It is neither trivial nor very accurate to use Eq. (2.17) as a basis for calculating the flux surface averaged $j \times B$ – torque profile which is of more interest, e.g. in transport modelling. A more useful form is obtained after noting that $B_\theta R = \nabla\Psi$ and that $j_{\text{fast}} = Zenv_r = Zen \cdot \dot{r} = Zen \cdot \dot{\Psi}/\nabla\Psi$ where Ψ is the poloidal flux and the dot means a time derivative. Using these identities the $j \times B$ – torque contribution is turned into a much better suited 1D form for diagnostics purposes

$$\tau_{j\times B} = -Zen\dot{\Psi}. \tag{2.18}$$

This quantity together with the collisional torque $\tau_{col} = m\Delta v_\phi R$ is used in ASCOT to estimate the total torque from fast ions into the plasma. Note that the ripple torque, which is related to the ripple induced radial current, is also captured by Eq. (2.18).

2.5 Momentum transport

Beyond analysing the ripple induced losses of torque and power, the accurate information of these quantities can be used to probe transport properties of the plasmas. In particular the evaluated torque is used to aid analysis of the toroidal momentum transport in JET plasmas. It has been shown both experimentally

[49–54] and theoretically [55–57] that momentum transport in fusion relevant tokamak plasmas is not purely diffusive but that convection also plays a role. Furthermore, although presently not very accurately quantified, momentum transport is affected by a term that is neither diffusive nor convective, thus named as the residual stress [58]. The equation governing the momentum transport in tokamak plasmas can be approximately written as [56, 59]

$$mnR\frac{\partial V_\phi}{\partial t} = \nabla \cdot \Gamma_\phi + S \tag{2.19}$$

where

$$\Gamma_\phi = mnR\left(\chi_\phi \nabla V_\phi + V_{pinch} V_\phi\right) + \Pi_{res} \tag{2.20}$$

is the toroidal momentum flux, V_ϕ is the toroidal velocity of the plasma, S is the torque source (e.g. NBI), χ_ϕ is the momentum diffusion coefficient, V_{pinch} is the convective coefficient (pinch velocity) and Π_{res} is the residual stress (the remaining part that is neither convective nor diffusive) and m, n, R are the mass, density and major radius, respectively. All terms, except mass and major radius, appearing in the above equations are functions of minor radius.

Experimentally the level of momentum transport has been observed to exceed the neo-classical level by a large factor [60–63]. Transport of momentum, like that of density or temperature, is indeed usually dominated by turbulent processes [56, 59, 64, 65]. Although much progress has been achieved in recent years to understand the processes responsible for the transport it is not possible to precisely predict the rotation even in simple L-mode plasmas. Experimental inter-machine scaling has been set up [66] but it fails to explain several observations [28]. Experimental analysis of the transport profiles χ_ϕ, V_{pinch} and the residual stress Π_{res} are thus necessary to validate the theory and to gain insight of the processes.

With many unknowns and only one differential equation Eq. (2.19) to use, special experimental arrangements are required to extract unambiguous information. In JET, the balanced neutral beam injection cannot be done due to the beamline geometry and momentum transport analysis is limited to cases where the residual stress term can be neglected. In such scenarios there are two ways to tackle Eq. (2.19). Either one looks at steady state rotation where one is left with an algebraic equation $\nabla \cdot \Gamma_\phi = -S$ with two unknowns, χ_ϕ and V_{pinch}, and is limited to estimating statistically the average transport across a number of dis-

charges (Publication III). Alternatively, one may use the information contained in the dynamical response of the plasma and make perturbation experiments where the torque source is modulated to perturb the rotation. In this case one can resolve the χ_ϕ and V_{pinch} profiles unambiguously [67].

2.5.1 NBI modulation technique

Modulation technique is a powerful experimental method for analysing various aspects of tokamak plasmas. It has been used on many tokamaks and using various modulated quantities (ECRH, ICRH, NBI, gas) e.g. [68–71]. NBI modulation, when properly executed, can be most useful for analysing momentum transport properties of plasmas. There are a number of criteria that must be met to be able to deduce χ_ϕ and V_{pinch} from the experiment. First, the target plasma to study needs to be quasi-stationary, i.e. the density, temperature and rotation should not drift or oscillate too strongly so that one can assume that the transport is the same during the time window of interest. The plasma should be MHD quiescent or at least the MHD effects should be non-interfering. Sawteeth oscillations in the core plasma or ELMs near the edge can sometimes be too strong or their frequency can get synchronised with the NBI modulation frequency to cause spurious rotation response and invalidate the data. Often the best target plasmas for the momentum transport analysis are in the low density L-mode regime or in H-mode where ELMs are absent and current profile can be tweaked to avoid sawteeth oscillations [72, 73]. Finally, the rotation measurement itself must have sufficiently good temporal and spatial resolution to resolve the dynamic plasma response accurately. In JET all these requirements are met easily after the CXRS upgrade [74].

In Fig. 2.11 the characteristic time traces of central signals are shown for a typical JET NBI modulation experiment. Plasma density, temperature, rotation and q-profile are the main parameters that determine the level of turbulent core transport and thus their modulation amplitude should remain as low as possible. The fact that the plasma in question is very stable and MHD free can be indirectly seen in the neutron measurement, which is dominated by the beam-thermal reactions; the amount of neutrons follows the NBI power waveform to the detail indicating very stable conditions. The NBI modulation frequency and amplitude have been chosen so that a sufficient perturbation ($\gtrsim$5%) in rotation is obtained

while simultaneously the density modulation is below noise level and only a limited response in ion and electron temperature is induced (typically $\lesssim 4\%$).

Note that as explained in Section 2.5.1 there are two mechanisms to transfer momentum from fast ions to the bulk plasma and they operate on different time scales; collisional torque on collisional timescale ($t \sim 100$ ms) and $j \times B$ – torque appearing almost instantaneously ($t \sim 100 \mu$s). Since the modulation cycle is shorter than the collisional time in JET it is usually the $j \times B$ – torque that is responsible for the majority of the rotation modulation amplitude. Since there are no corresponding fast mechanisms to transfer energy, at least in significant magnitudes, the modulation amplitude for temperature is automatically smaller helping to achieve sufficient rotation modulation while keeping the plasma otherwise in steady condition.

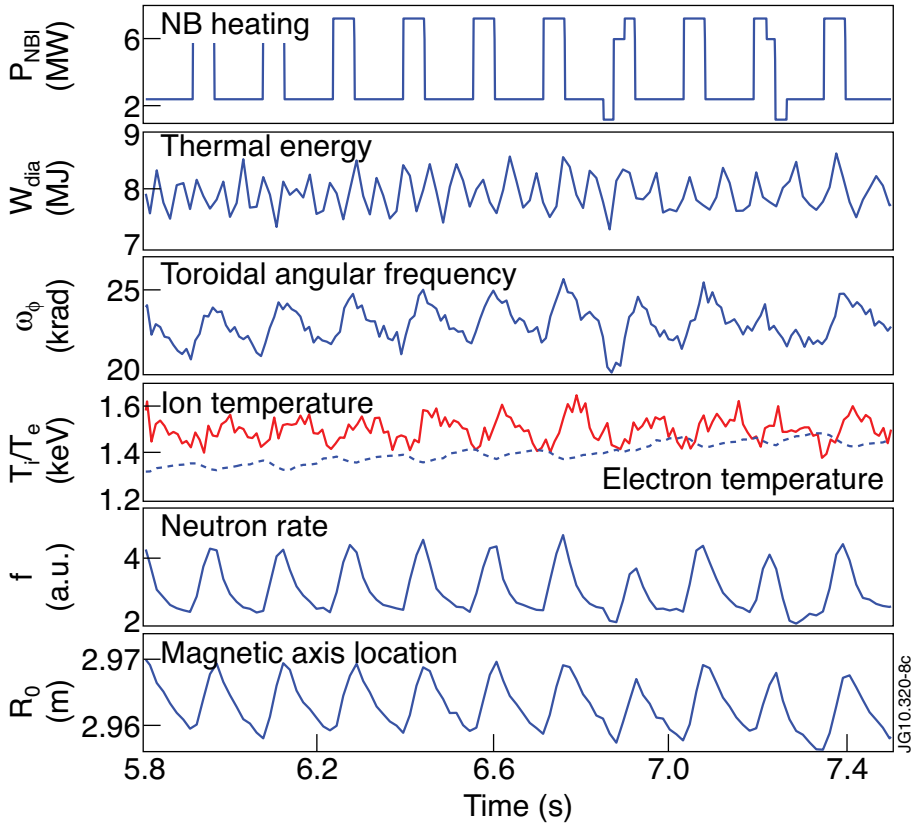

Figure 2.11. Time traces of relevant parameters in a typical momentum transport experiment in JET (#77089) utilising NBI modulation to perturb the plasma. (from Publication V)

In order to find out the prevailing momentum transport in the experiment one

can, e.g. use an iterative procedure where: (1) a transport solver is used to solve the Eq. (2.19) for V_ϕ with given profiles of χ_ϕ and V_{pinch}, (2) resulting rotation response is compared against the measured rotation and (3) χ_ϕ and V_{pinch} profiles are modified until agreement is found [67]. In Publications V–VI this procedure was automated using JETTO transport code for step 1, Fourier amplitude and phase profiles together with steady state rotation data for step 2 and a MatLab based non-linear minimisation algorithm for step 3.

3. Tools and methods

The type of work presented in this thesis consists of computer simulations and simulation aided analysis and interpretation of JET experimental data. Computer simulations are the bridge between theory and experiments and can give an idea whether the theoretical understanding (as it is implemented in the codes) of the physical phenomena is correct or whether some additional mechanisms are needed to explain the experimental data. The overall task has been to understand the fast ion behaviour in the plasma (in quiescent MHD conditions), to evaluate fast ion heat and torque sources for studying the bulk plasma properties and to validate the theory and the tools used. The difficulty lies in getting quantitative and accurate numbers from the codes that can be compared with experimental observations. This effort involves the use and development of both new and existing tools and methods to do the analysis. The most important tools and modifications to them are shortly introduced in the following.

3.1 ASCOT code and upgrades

ASCOT [75, 76] (**A**ccelerated **S**imulations of **C**harged particle **O**rbits in **T**ori) is a guiding centre following code with Monte Carlo operators for added physics, developed from the early 90's in VTT (Technical Research Centre of Finland) and Aalto University (formerly HUT, Helsinki University of Technology).

The standalone ASCOT is primarily used for fast particle studies where the particle ensemble of interest can be treated as a tracer species which does not self-interact or modify significantly the plasma itself. Monte Carlo techniques are used to add physics such as Coulomb collisions or ICRH interactions [77]. Many interesting and complicated fast particle physics can be studied with ASCOT by

simply imposing a realistic three dimensional magnetic perturbation, e.g. toroidal field ripple[78], NTMs [79, 80] or external perturbation coils [81–83] on top of the equilibrium field. The advantage of the orbit following MC codes such as ASCOT is that it is straightforward to study many interconnected and complex phenomena by adding MC operators on top of each other. For comprehensive details of ASCOT the reader is referred to the earlier work [84, 85] where more elaborated description of the equations of motion, collision operator etc. can be found.

As part of this thesis ASCOT has been upgraded to calculate the torque on the plasma coming from fast ion radial transport as described in Section 2.3.1. This supplied ASCOT with a unique feature within the orbit following codes in the world: a possibility to calculate fast ion ripple torque in real experimental condition. The torque evaluation feature has been utilised on several occasions, with and without ripple, to estimate fast ion torque and its influence on plasma rotation. Furthermore, ASCOT was integrated into the JET application management system (JAMS), featuring a graphical user interface, and to relevant codes within it to facilitate the JET NBI modelling capability. Without these and related code enhancements much of the subsequent results could not have been obtained.

3.2 JET integrated transport code

JET integrated transport code (JINTRAC) is a transport solver used at JET. At the core of JINTRAC is a 1.5D transport code JETTO [86] which solves a set of differential equations for flux surface averaged plasma density, temperature and momentum. The half a dimension is credited by the inclusion of plasma shape information through the flux surface averaging. For solving the time evolution of the plasma parameters JETTO is coupled to various models and sophisticated codes (incl. ASCOT) to provide information on transport, sources and magnetic equilibrium [87]. The integrated code can then be advanced sequentially to yield a consistent evolution of plasma density, temperature and rotation. A schematic overview of the system is shown in Fig. 3.1.

The evolution of density, temperature and momentum are coupled together (e.g. increasing density means less available power per particle which results in lower temperature and so on) and for full solution a coupled set of differential equa-

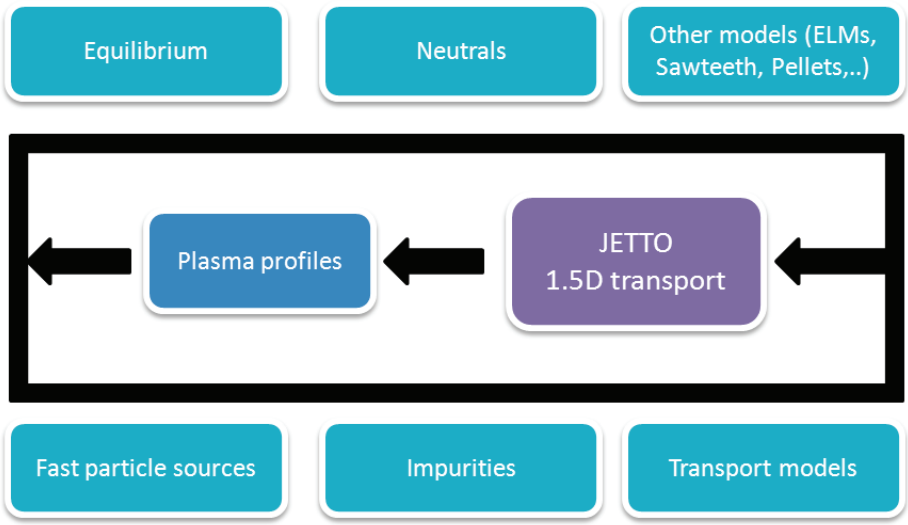

Figure 3.1. Schematic view of the JINTRAC operation. The modules for equilibrium, neutrals etc. feed information for the transport code JETTO that calculates the evolution of the plasma profiles based on their input. The plasma profiles are input for the modules which then evaluate the next round of input for JETTO. ASCOT is included in the Fast particles sources box.

tions need to be solved. JINTRAC can be used both in predictive and in interpretative mode. In predictive mode the transport coefficients (e.g. χ_ϕ and V_{pinch}) are given by the user, by some model or theory together with initial and boundary conditions and the evolution of plasma profiles are obtained. In interpretative mode JINTRAC takes the time histories of experimentally measured plasma profiles together with the calculated sources to yield the effective diffusion coefficients for momentum, temperature and density. The effective momentum diffusion coefficient $\chi_{\phi,\text{eff}}$ for example is obtained through the momentum flux $\Gamma_\phi = mnR\chi_{\phi,\text{eff}}\nabla V_\phi$ i.e. it assumes all flux is caused by diffusion. The predictive mode can be used in an iteration loop to fit the transport profiles that best reproduce the experimental measurements (see next Section).

During the course of this work JINTRAC was upgraded with a new module to provide a more accurate description of the NBI source. The module is based on ASCOT which was adapted for time dependent use and interfaced with relevant JINTRAC modules and experimental database. ASCOT became an important module within the box labelled as Fast particle sources in Fig. 3.1. This upgrade made it possible to calculate a realistic NBI deposition profile with either experimental or user defined NBI characteristics (power, energy, PINI mix) and to take

into account all relevant neoclassical physics from large orbit effects to charge exchange (CX) losses with appropriate dynamics.

3.3 Momentum transport analysis technique

In order to deduce the prevailing transport properties from experimental plasma we have developed an automated iterative scheme around JINTRAC using MatLab tools. For enabling this scheme a special version of JINTRAC was first made which allows externally provided radial profiles of χ_ϕ and V_{pinch} to be used in the predictive momentum transport simulation. Within the MatLab code JINTRAC was called repeatedly to provide the predicted toroidal rotation corresponding to the given χ_ϕ and V_{pinch} profiles. The objective is to vary these profiles until the best fit between the simulated toroidal rotation and the experimentally measured toroidal rotation is found. For finding the optimal profiles efficiently a built-in MatLab non-linear optimisation algorithm was employed.

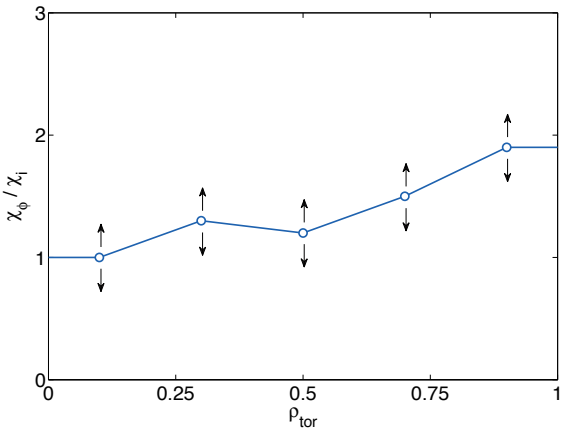

Figure 3.2. An example of profile parametrisation for finding the optimal transport profiles. The free parameters are connected by linear interpolation. The values at the boundaries are fixed to the closest point being optimised. The vertical arrows indicate that the values at the node locations are varied until the optimum profiles are found.

Although it seemingly is a simple task to find the optimal transport profiles to best match the experimental measurements, there are a couple of caveats that need closer attention. First of all, profile optimisation is an inherently multi-dimensional problem the dimensions being the sum of parameters needed to con-

struct the profiles. We chose to represent the profiles with 3 to 6 discrete points equispaced in radius with linear interpolation in between as illustrated in Fig. 3.2. This gives a 6 to 12 dimensional space to be scanned (using 2 profiles). It is rather obvious that in a multi-dimensional system several local minima can exist. To improve the robustness of finding the best fit (global minimum) the minimisation algorithm is run several times each with random initial condition. To speed up convergence and the likelihood of finding physically relevant profiles a certain level of smoothness was required of the transport profiles by penalising large second derivatives. Finally, it should be mentioned that not all problems like these can be solved uniquely. It is a matter of each individual case to check if such situation exists. Fortunately, the repetition of the optimisation with several randomly chosen initial conditions usually helps in the identification process.

3.4 ICRH modelling tools

Ion cyclotron resonance heating (ICRH) is in many ways a very complicated process to simulate [26]. For instance the absorption efficiency depends on the resonant ion distribution (in space and velocity space) both of which change during the heating, i.e. the process is non-linear unlike NBI in most relevant cases. The codes for ICRH are typically very specialised and require a self-consistent time-dependent treatment. In the future some recent work [77, 88] on ICRH theory is expected to provide orbit following codes such as ASCOT the capability to simulate ICRH as part of the integrated tokamak modelling (ITM) suite [89]. Present ICRH modelling work, however, is based on PION [90, 91] and FIDO [92] codes, described in the following.

PION is a simplified Fokker-Planck code for ICRH modelling. It is routinely used in JET and it has been extensively benchmarked against JET ICRH experiments (see e.g. [90, 91]). Unlike most of the ICRH codes PION is rather fast taking only from a few minutes to few hours to calculate the heating profiles from ICRH for the complete heating phase which can be over 10 seconds. PION solves the evolution of the pitch angle averaged fast ion distribution function f

$$\frac{\partial f}{\partial t} = \hat{C}(f) + \hat{Q}(f) \tag{3.1}$$

using finite differencing method. Here $\hat{C}$ is the collision operator and $\hat{Q}$ is the

quasi-linear RF diffusion operator [24] with an RF diffusion coefficient

$$D_{RF} \sim |E_+ J_{\mathrm{n}-1}(k_\perp v_\perp/\Omega_{ci}) + E_- \mathrm{J}_{\mathrm{n}+1}(k_\perp v_\perp/\Omega_{ci})|^2 \tag{3.2}$$

where $E_+(E_-)$ are right (left) hand polarised electric field components, $k_\perp$ and $v_\perp$ is the perpendicular wave number of the fast wave, n is the harmonic number of the resonance and J_m are the Bessel functions of the first kind.

PION is a simplified code with a number of limitations and it cannot output detailed information of the resonant ion distribution function. However, in several common heating scenarios it has been shown to accurately predict the ICRH power absorption and the resulting fast ion energy content [93, 94]. In the work done for Publication I the role of PION is to provide the amount of energy absorbed by the resonant species as well as to calculate the ICRF antenna power spectrum to be used with the more sophisticated ICRH code FIDO.

FIDO solves the orbit averaged Fokker-Planck equation Eq. (3.1) using Monte Carlo methods [95, 96]. It goes one step further in orbit averaging than ASCOT. Where ASCOT follows the location of the guiding centre FIDO keeps track of the invariants of motion $(\tilde{E}, \Lambda, \tilde{P}_\phi)$ which are normalised versions of the invariants presented in Eqs. (2.4-2.6). In effect FIDO averages also over the poloidal motion of the particle. The collisions and RF interactions are modelled by Monte Carlo kicks in the invariant space. This approach has the obvious benefit of being much less CPU intensive than the guiding centre approach since the poloidal motion of the particles is not followed. Nevertheless, FIDO simulations last from several hours to several days even in massively parallel computing environment due to the large number of particles needed to accurately represent the high energy tail in the fast ion distribution.

For running FIDO the user must give the power spectrum of the fast wave as input such that it produces a correct amount of absorbed power. The shape of the spectrum is determined by the geometry of the antenna and the phasing between the current straps but the amplitude is often not known in advance. For this reason PION is used, as mentioned above, to provide the amount of power absorbed by the resonating ions. The power spectrum used in FIDO can then be normalised using an iterative procedure. Usually already one or two iterations will produce an accurate power absorption in FIDO. In the end FIDO delivers detailed information of the fast ion distribution function which can be compared

with experimental measurements such as the measurement from the neutral particle analyser (NPA) [97] in Publication I.

4. Results

4.1 Fast ion energy diffusion barrier confirmed in modelling

Quasi-linear theory predicts an effective energy diffusion barrier near $E = E^*$ where the RF diffusion coefficient D_{RF} in Eq. (2.12) has its first minimum. In order to test experimentally the validity of the prediction a dedicated experiment was planned on JET. The motivation for this work as reported in Publication I was the experimental validation of the theory and the benchmarking of the existing ICRH codes (FIDO/PION). The best suited ICRH scenario for this experiment was found to be the second harmonic heating scheme. Firstly, it allows to use low enough toroidal magnetic field ($E^* \sim B^2/n_e$) to put the energy diffusion barrier in the energy range where it can be measured by the neutral particle analyser (NPA) [97]. NPA measures the escaping fast neutrals from about 200 keV up to around 1.2 MeV (depending on species). Fast neutrals are born in charge exchange reactions between cold neutrals and fast ions which, in the presence of ICRH, are dominantly the resonant species and can thus yield a representative description of the ICRH accelerated ion population. Secondly, the second harmonic scheme is more efficient than higher harmonic heating schemes at low energies to pull out a high energy tail [98].

To test this theory, three plasma discharges were utilised to make two pairwise comparisons. First pair is a low density & low power plasma versus a high density & high power plasma. The purpose here is to vary the location of the barrier E^* via density variation while maintaining equal heating power per particle by having more ICRH power in the high density discharge. The second pair is formed between discharges with equal density but with different heating power. In this

case, if the quasi-linear theory is valid, similar shaped fast ion tail would develop in both discharges. Otherwise, the significantly higher heating power per particle would lead to a markedly longer tail in the energy distribution.

Fig. 4.1 shows the NPA measurements together with FIDO/PION simulation of the fast ion energy distribution for these discharges. It is apparent that the modelling agrees well with the measurements and that they both show distributions which drop rapidly at high energies. In the first harmonic ICRH heating scheme the resonant ion energy distribution would usually decay exponentially forming a straight line in the logarithmic plot. Here the fast ion population decreases increasingly faster towards higher energies which is expected from the quasi-linear theory at this range of parameters. Furthermore, by comparing the discharges #58738 and #58739 (low power v. high power) one can see that the shapes and the fall-off energies of the distributions are same as expected from quasi-linear theory. Comparison between discharges #58734 and #58738 (high density v. low density) also agrees with the theory as with similar heating power per particle the distribution falls off earlier in the high density discharge. For additional pairwise comparison of experimental data, see Publication I, Fig. 4.

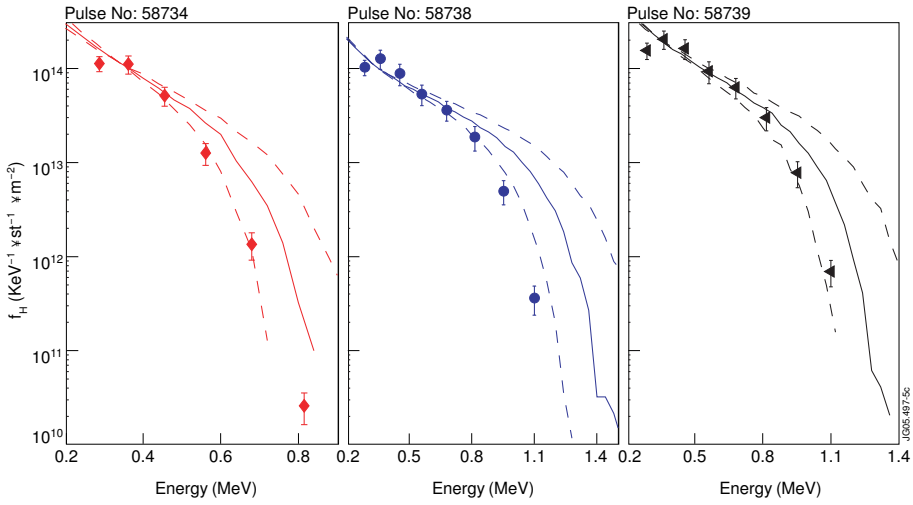

Figure 4.1. Comparison of the measured and simulated fast ion energy distributions in second harmonic hydrogen minority ICRF heated plasmas. a) high power & high density b) low power & low density c) high power & low density. Points with errorbars are the experimental measurements, full lines are the simulated distributions and dashed lines indicate the sensitivity of the simulations to 10% change in electron density (from Publication I).

4.2 Fast ion ripple torque calculation using the orbit following code ASCOT

Toroidal field ripple, as described in Section 2.3.1, can have a significant impact on plasma performance and thus it can influence the economics of fusion power. In the ITER design the number of toroidal field coils has been fixed to 18 which could cause ripple as high as 1.2%. In order to help to assess the consequences that might result from this large level of ripple, JET launched a dedicated experimental ripple campaign C18 to study its effect on, e.g. the plasma confinement, H-mode threshold, ELMs and fast ion losses. The key ingredient for the campaign, unique to JET, is its ability to control the level of ripple by driving unequal currents in even and odd numbered TF coils. This allows isolating the influence of ripple by running identical discharges where only the level of ripple is changed.

While it is relatively easy to show from the experimental data that ripple influences the plasma characteristics the quantitative understanding of these observations requires validated tools that are able to take into account the effect of ripple. To support the analysis of the experimental data ASCOT code was upgraded as a part of this thesis so that the influence of TF ripple on fast ion torque and losses could be estimated. In short, this work involved interfacing the orbit following ASCOT with PENCIL [99] code to obtain the 3D ionisation source of the JET neutral beam system. With this source ASCOT was used for the slowing down simulation during which the orbit losses and ripple effects occur. Furthermore, torque diagnostics were added to calculate the total torque from the injected NBI so that it includes both the slow collisional torque and the instantaneous $j \times B -$ torque.

As a result of the ASCOT implementation work the first ASCOT analysis of JET NBI torque in presence of magnetic field ripple was reported in Publication II. It was shown that the NBI torque, which in JET is normally in co-current direction, is significantly reduced by the ripple when the magnitude of the ripple increases above $\delta > 0.35\%$ (see Fig. 4.2).

This observation was consistent with the experimental data that showed little effect from ripple if $\delta < 0.35\%$ [100]. One somewhat surprising finding from the simulations was that the counter torque in JET was mainly generated by the radial ripple diffusion of the poloidally trapped ions instead of the losses of the toroidally trapped ions. According to ASCOT simulations the ripple trapping in

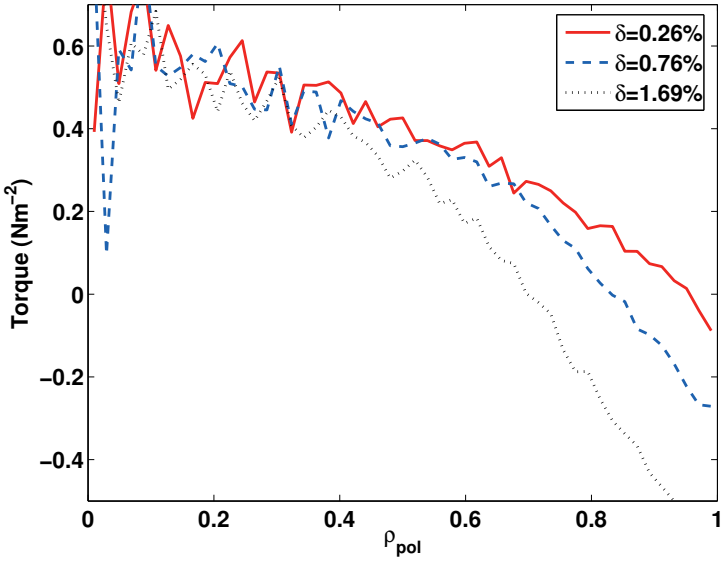

Figure 4.2. NBI torque profile for three different ripple magnitudes δ. Note how the magnitude of the negative (counter-current) torque increases towards the separatrix while the torque inside mid radius is unaffected even at the highest ripple (from Publication II).

JET becomes significant in NBI heated plasmas only at ripple levels larger than 1.5%. This was good news also because the areas where the ripple trapped ions hit the first wall are not well protected and therefore material melting could result more easily.

4.3 Fast ion ripple torque influence on plasma rotation

As an application of the newly obtained torque calculation functionality a mixture of H-mode experiments were analysed with ASCOT. The various plasmas had different density and temperature profiles as well as a broad selection of NBI heating power and alignment. Most of these plasmas were run with 1% ripple. The toroidal rotation in these plasmas was compared with the ASCOT calculated torque as shown in the Fig. 4.3. It was found that the fast ion ripple torque, which always points in the counter current direction, reduces the NBI torque significantly and depends on the alignment and deposition profile. With 1% ripple and perpendicular NBI the fast ion ripple torque can in some cases result in a counter current torque that completely cancels the NBI torque. The measured

total toroidal angular momentum of the plasmas correlates well with the ASCOT calculated torque suggesting that fast ions are responsible for the major part of the ripple generated toroidal torque.

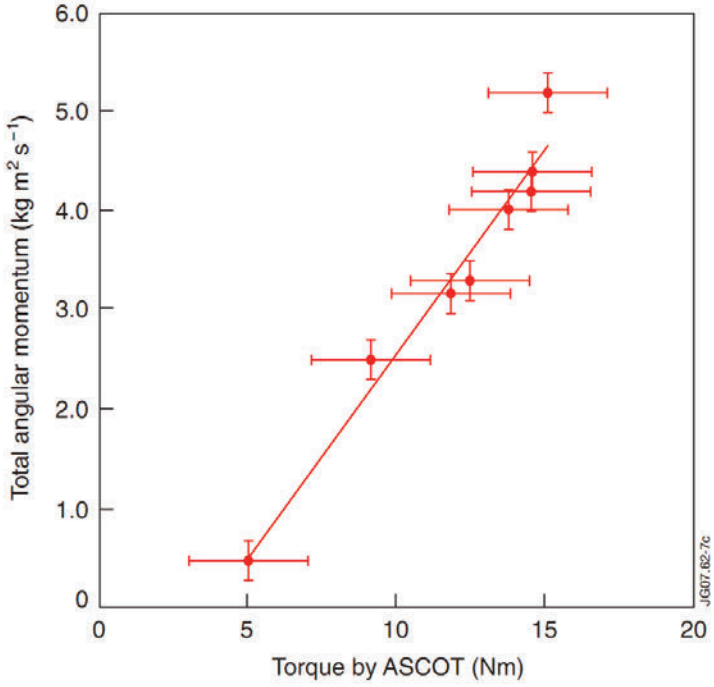

Figure 4.3. The measured total angular momentum versus ASCOT calculated NBI torque in presence of TF ripple (from Publication III).

However, it was also found that for some plasmas the edge region was rotating in counter current direction while ASCOT still predicted positive co-current total torque. This could signify an unaccounted missing torque contribution. One possible explanation for the observation is a contribution from thermal ions, e.g. neoclassical toroidal viscosity (NTV) as demonstrated in DIII-D [20].

4.4 Momentum transport in NBI heated JET plasmas

Toroidal rotation of the plasma is controlled by the momentum sources, e.g. NBI, and the radial transport of the momentum as given by Eq. (2.20). With the accurate knowledge of the sources, using codes like ASCOT, and the measured toroidal rotation, information of the momentum transport can be obtained experimentally with different approaches as described in Section 2.5.

The statistical approach was used in Publication III where the toroidal rotation of a number of JET discharges were analysed. Here only the steady state information of rotation and sources were used and the left hand side of Eq. (2.19) vanishes and momentum flux is obtained by simply integrating the known steady state source over the plasma volume $\Gamma_\phi = \int dvS$. Neglecting the residual stress and denoting the angular momentum density as $\Omega = mnRV_\phi$ the Eq. (2.20) can be written as

$$\frac{\nabla\Omega}{\Gamma_\phi} = -\frac{V_{pinch}}{\chi_\phi}\frac{\Omega}{\Gamma_\phi} - \frac{1}{\chi_\phi} \tag{4.1}$$

Since the terms $\nabla\Omega$, Ω and Γ_ϕ can be measured or calculated the unknowns χ_ϕ and V_{pinch} can now be obtained statistically.

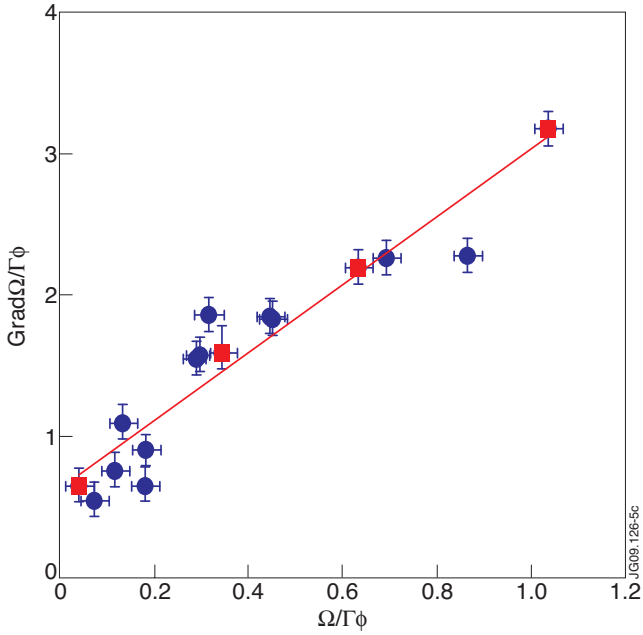

Figure 4.4. Normalised momentum density gradient versus normalised momentum density for a number of JET H-mode discharges. Square markers are ones from a ripple scan (from Publication IV).

In Fig. 4.4 the normalised gradient of the angular momentum density $\nabla\Omega/\Gamma_\phi$ is plotted against the normalised angular momentum density Ω/Γ_ϕ for a number of different discharges. The values shown are obtained at mid radius. By fitting a line into the scatter plot one can obtain the ratio V_{pinch}/χ_ϕ from the slope and $1/\chi_\phi$ from the crossing of the y-axis. It should be repeated that using this method based on steady state form of Eq. (2.19) only the average pinch velocity

and momentum diffusion coefficient across the discharges can be obtained. Nevertheless, by repeating the analysis for additional radial positions it was found that the magnitudes and trends of the radial profiles for χ_ϕ and V_{pinch} are similar than previously found using NBI modulation technique for low density L-mode plasmas [52]. The work thus not only confirms the earlier analysis but also shows that a non-zero convective momentum transport V_{pinch} is robustly found in large data sets and that similar processes are at play universally across various plasma conditions.

4.5 Experimental validation of the fast ion ripple torque calculation

While in earlier Publications the NBI torque in presence of TF ripple was calculated and used in further analysis, it was not until Publication V that it could be validated experimentally. The earlier efforts to validate the guiding centre following approach to account the ripple effects were limited to comparing quantities that did not include torque either because experimental data was not available or no other code could calculate the ripple torque. Nevertheless, other ripple effects have been successfully validated earlier, e.g. ripple induced fast ion heat loads on first wall have been compared against experimental data deduced from infra-red measurements [101, 102].

The main problem of validating the torque calculation arises nevertheless from the fact that the torque itself cannot be measured. Torque can only be inferred from Eqs. (2.19) and (2.20) when the rotation profile is measured and the transport is known. However, as discussed earlier, only two unknowns can be deduced experimentally from Eqs. (2.19) and (2.20) even with the dynamic information kept. With the addition of a significant TF ripple, the NBI torque source S itself becomes unknown. One is thus left with too many unknowns to solve from a single equation. The way forward from the apparent dead end is to design an experiment with negligible residual stress for two nearly identical discharges; one without ripple and one with ripple. The data from the ripple-free discharge can be used to find χ_ϕ and V_{pinch} profiles as described in Section 2.5.1. Then, with the just resolved transport coefficients, toroidal rotation can be found for the plasmas with TF ripple using the torque calculated by ASCOT. Should the torque calculation be accurate, the experimental and calculated rotation profiles will be consistent.

In order to use this experimental approach to validate ASCOT ripple torque calculation the code first had to be upgraded for time-dependent operation to obtain $S(r,t)$. With this new functionality the NBI torque profile was calculated for three discharges (#77089-#77091) with nearly identical plasma profiles. Ion and electron temperature and density profiles as well as the q-profiles were identical within the measurements accuracy and the density profiles differed less than 10% between the discharges. The calculations used a time resolution of 5 ms to obtain good statistics and sufficiently accurate dynamic information of the torque sources. The torque profiles as calculated by ASCOT were markedly different between the discharges (see Fig. 11, Publication V) in line with expectations and thus provide a nice set of data for validation.

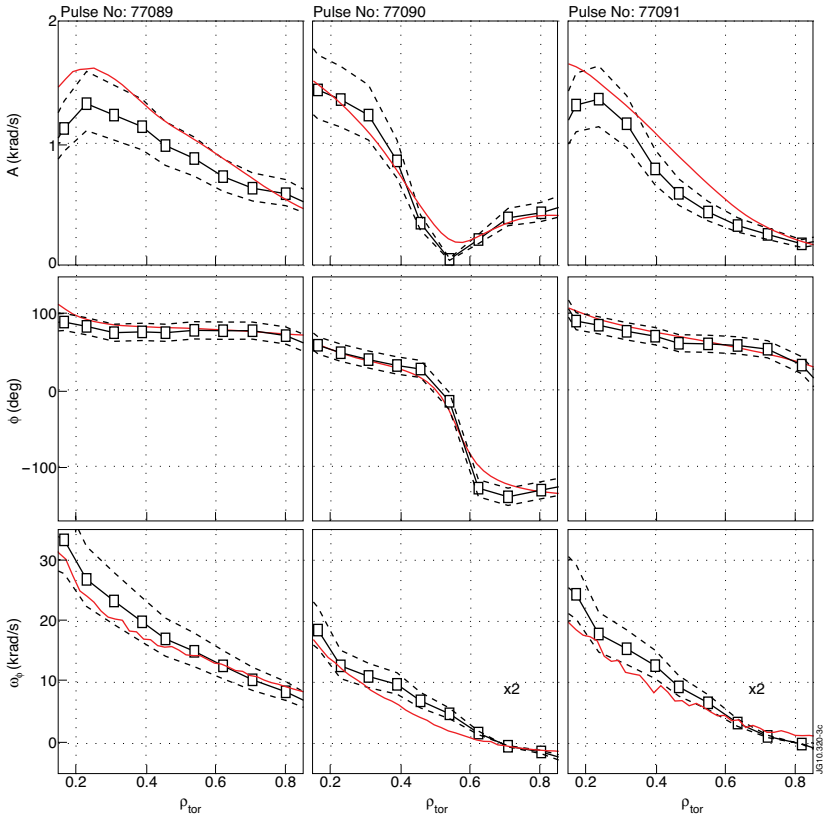

Figure 4.5. Amplitude, phase and steady state profiles for toroidal rotation (red = calculations, black = measurements). First column corresponds to the discharge #77089 ($\delta = 0.08\%$, perp. NBI), second column to #77090 ($\delta = 1.5\%$, perp. NBI) and third column to #77091 ($\delta = 1.5\%$, tang. NBI). Dashed lines are to guide the eye and give rough estimates of the error (from Publication V).

Using the procedure outlined above and in Section 2.5.1 the momentum transport profiles were iteratively solved for the reference discharge without ripple (#77089). With the transport found this way together with the ripple torque calculations the transport code predictions and experimental rotation measurements could be compared. Figure 4.5 gives the final result of this procedure. The left column shows the Fourier amplitude and phase at the 6.25 Hz modulation frequency together with the steady state rotation profile for the reference discharge without ripple. The middle and the right columns show the same data for the discharges with 1.5% ripple. Perpendicular NBI was used in the discharge #77090 whereas tangential NBI was used in #77091. In all plots one can see that the simulated rotation with torque calculated by ASCOT (red lines) agrees well with the experimentally measured toroidal rotation profiles (black squares) which suggest that the torque is evaluated correctly. The dashed lines give indication of the measurement errors in the rotation data. The plots also show that the counter current torque from ripple is significantly larger in the case of perpendicular NBI injection in line with the theoretical expectations.

It should be mentioned that although the ripple effect has been found to be strongest for fast ions both in theory and in simulations, the introduction of non-axisymmetric perturbations also affects thermal particles through the neoclassical toroidal viscosity (NTV) [36–40]. While there is experimental evidence showing that this effect is important with certain excited low toroidal harmonic perturbations [20] there have not been experimental observations that suggest that this effect would be particularly strong in the JET TF ripple field.

4.6 Parametric study of momentum transport using NBI torque modulation

The torque from NBI ions can be used to gain information of the momentum transport properties of the plasmas as explained in Sec. 2.5.1. The key ingredient here is the ability to accurately calculate the torque. NBI modulation technique has been used previously to show that momentum transport is not purely diffusive, as expected from the characteristics of the ion energy diffusion, but that a convective term also plays a role [51, 52]. In Publication VI momentum transport and in particular its convective part (pinch) is studied using the NBI modulation technique in JET plasmas. The aim is to find out how the pinch depends on plasma

parameters in an effort to make predictions for ITER. The importance of this topic is realised when noting that even a relatively small level of pinch in ITER could provide a mechanism for achieving a sufficient level of rotation to mitigate turbulence [103] and to avoid harmful mode locking and subsequent disruptions [20].

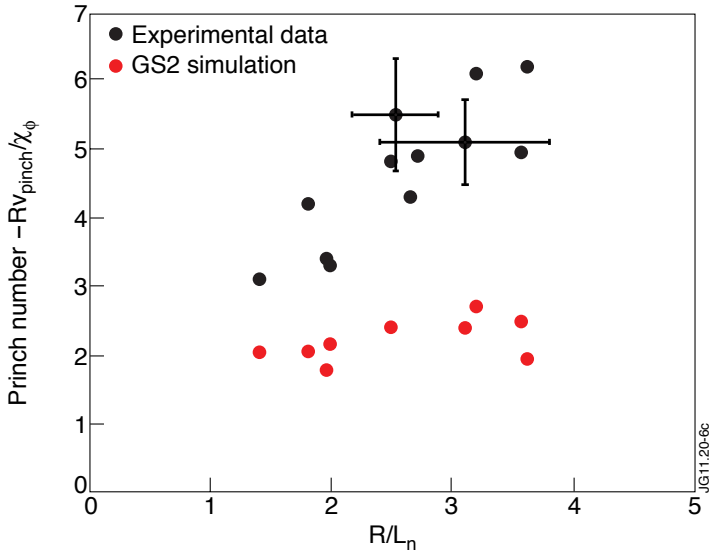

Figure 4.6. Comparison between experimental and numerical scaling of the pinch number RV_{pinch}/χ_ϕ against the inverse of the normalised density gradient scale length (from Publication VI).

The dependencies of the pinch on plasma parameters are studied by making a series of NBI modulation experiments with as wide parameter range as possible. The theoretically motivated parameters of interest that are varied are the q-profile, collisionality and the density gradient (more specifically the inverse of the normalised density gradient scale length $R/L_n = R\nabla n/n$) [56]. The experimental profiles for χ_ϕ and V_{pinch} are deduced using the iterative transport analysis based on JINTRAC (Sec. 2.5.1) with NBI torques calculated using well agreeing codes TRANSP [104] and/or ASCOT. It is found that the variation of pinch against q and collisionality is weak while the dependence with the R/L_n is strong. The weak dependence on the collisionality agrees well with the theory based modelling [105]. Figure 4.6 shows the pinch number against the inverse of the density gradient scale length for the experimental and numerical data from turbulence simulations using GS2 [106] code in linear mode. Linear simulations are thought to be sufficiently accurate for momentum transport analysis in ITG dominated plasmas

where they agree quite well with non-linear simulations [107–110]. Both experimentally and in simulations the pinch number increases with R/L_n although the dependence in the experimental data is clearly stronger (by roughly a factor or three). The reason for this difference is not yet understood and it requires more analysis to resolve. The result suggests that peaked density profiles could help ITER to achieve higher rotation and rotation shear even with the weak external torque sources in the plasma core.

5. Summary and discussion

Fast ions have several important roles in fusion plasmas. The 3.5 MeV alpha particles born in the D-T fusion are crucial in order to maintain the high temperature required for the fusion to occur while NBI+ICRF ions are needed to heat up the plasma during the start-up phase and to control the plasma burn. Understanding the generation of fast ions as well as the mechanisms that control their losses and distribution in the plasmas is important in order to successfully operate future fusion power plants. Furthermore, the accurate fast ion modelling capability makes it possible to use them as a tool for studying the bulk plasma properties.

Ion cyclotron heating is currently seen as the best option for heating bulk ions into the optimal 10–20 keV energy range for fusion burn in ITER. In this work, a prediction from the quasi-linear theory was tested with ICRF codes PION and FIDO. According to the theory the RF diffusion coefficient becomes small at certain energies due to the finite Larmor radius effects which is expected to manifest itself by strongly decaying fast ion tail around this energy. Simulations of this phenomenon agreed well with the experimental measurements and confirmed the importance of the finite Larmor radius effects in controlling the fast ion distribution function. This effect allows one to have some control over the tail of the ICRF heated fast ion distribution by adjusting the magnetic field strength and the electron density as required by the experiment.

During the course of this thesis the orbit following Monte Carlo code ASCOT code has been upgraded to calculate the fast ion torque to the plasma with and without ripple. ASCOT was also modified for time-dependent calculations which is crucial for analysing, e.g. the NBI modulation experiments. Furthermore, ASCOT was integrated into the JAMS (JET Application Management System) and interfaced with JETTO and experimental database to allow routine analysis of

NBI heated discharges at JET. A realistic fast ion ripple torque in presence of collisions and true geometry was first calculated with ASCOT.

The numerical analysis of fast ion losses and the effect of ripple on rotation in the JET ripple campaign have contributed in the ITER design recommendation that calls for a reduction of the ITER intrinsic ripple magnitude $\delta \sim 1.2\%$ to as low as reasonably achievable [111]. This could be achieved using in-vessel ferritic inserts (steel plates) [112] similar to as already demonstrated in JFT-2M and JT-60U [113–115]. Both ASCOT simulations and JET experiments have shown that for $\delta < 0.3\%$ the fast ion ripple losses and counter current torque become small and that the deterioration of the plasma performance becomes insignificant.

NBI modulation technique with ASCOT calculated torque was used for studying the momentum transport properties of plasmas. It was shown that the convective momentum transport (inward pinch) is present in a broad range of NBI heated discharges and that it does not depend significantly of the plasma collisionality while a relatively strong dependence was found against the density gradient scale length L_N. The existence of such inward pinch could allow peaking of the rotation profile in ITER even with the expected weak momentum sources in the core plasma.

The NBI modulation technique was also utilised in an effort to experimentally validate the ripple torque calculations for the first time. It was found that the torque calculated by ASCOT did successfully reproduce the experimentally measured rotation confirming that the counter current ripple torque is accurately calculated with the guiding centre approach. Having an experimentally validated tool for taking into account fast ion ripple effects makes it possible to apply it for predictive analysis in ITER and beyond.

Bibliography

[1] *World energy outlook 2011*. IEA, International Energy Agency OECD, Paris, 2011. ISBN 978-92-64-12413-4, Online.

[2] *BP energy outlook 2030*. British Petroleum, London, 2012, Online.

[3] Tokamak. In *The Great Soviet Encyclopedia, 3rd Edition*.

[4] M. Keilhacker, A. Gibson, C. Gormezano, et al. High fusion performance from deuterium-tritium plasmas in JET. *Nuclear Fusion*, 39(2):209, 1999, Online.

[5] ITER Technical Basis 2002. ITER EDA. *Documentation Series No 24. (Vienna: IAEA)*, 2002, Online.

[6] ITER Organisation. `http://www.iter.org/`.

[7] K. Ikeda. ITER on the road to fusion energy. *Nuclear Fusion*, 50(1):014002, 2010, Online.

[8] J. Wesson and D.J. Campbell. *Tokamaks*. Oxford engineering science series. Clarendon Press, 1997. ISBN 9780198562931.

[9] K. Tobita, K. Tani, Y. Kusama, et al. Ripple induced fast ion loss and related effects in JT-60U. *Nuclear Fusion*, 35(12):1585, 1995, Online.

[10] M. H. Redi, R. V. Budny, D. S. Darrow, et al. Modelling TF ripple loss of alpha particles in TFTR DT experiments. *Nuclear Fusion*, 35(12):1509, 1995, Online.

[11] M. H. Redi, M. C. Zarnstorff, R. B. White, et al. Collisional stochastic ripple diffusion of alpha particles and beam ions on TFTR. *Nuclear Fusion*, 35(10):1191, 1995, Online.

[12] H. H. Duong, R. K. Fisher, S. S. Medley, et al. The effect of toroidal field ripple on confined alphas in TFTR DT plasmas. *Nuclear Fusion*, 37(2):271, 1997, Online.

[13] K. Miyamoto. *Plasma physics and controlled nuclear fusion*. Springer, Berlin New York, 2005. ISBN 9783540242178.

[14] V. G. Kiptily, F. E. Cecil, O. N. Jarvis, et al. γ-ray diagnostics of energetic ions in JET. *Nuclear Fusion*, 42(8):999, 2002, Online.

[15] D. S. Darrow, H. W. Herrmann, D. W. Johnson, et al. Measurement of loss of DT fusion products using scintillator detectors in TFTR (invited). *Review of Scientific Instruments*, 66(1):476–482, 1995, Online.

[16] S. Baeumel, A. Werner, R. Semler, et al. Scintillator probe for lost alpha measurements in JET. *Review of Scientific Instruments*, 75(10):3563–3565, 2004, Online.

[17] R. L. Miller and R. E. Waltz. On the nature of rotational shear stabilization in toroidal geometry and its numerical representation. *Physics of Plasmas*, 1(9):2835–2842, 1994, Online.

[18] K. H. Burrell. Effects of E x B velocity shear and magnetic shear on turbulence and transport in magnetic confinement devices. *Physics of Plasmas*, 4(5):1499–1518, 1997, Online.

[19] P. Mantica, D. Strintzi, T. Tala, et al. Experimental study of the ion critical-gradient length and stiffness level and the impact of rotation in the JET tokamak. *Phys. Rev. Lett.*, 102:175002, Apr 2009, Online.

[20] A. M. Garofalo, M. S. Chu, E. D. Fredrickson, et al. Resistive wall mode dynamics and active feedback control in DIII-D. *Nuclear Fusion*, 41(9):1171, 2001, Online.

[21] G. Duesing, H. Altmann, H. Falter, et al. Neutral beam injection system. *Fusion Technology*, 11(1):163–202, 1987, Online.

[22] Heating ITER Physics Expert Group on Energetic Particles, Current Drive, and ITER Physics Basis Editors. Chapter 6: Plasma auxiliary heating and current drive. *Nuclear Fusion*, 39(12):2495, 1999, Online.

[23] J. P. Freidberg. *Plasma Physics and Fusion Energy*. Cambridge University Press, 2008. ISBN 9780521733175.

[24] T. H. Stix. Fast-wave heating of a two-component plasma. *Nuclear Fusion*, 15(5): 737, 1975, Online.

[25] D. Anderson. Distortion of the distribution function of weakly RF heated minority ions in a tokamak plasma. *Journal of Plasma Physics*, 29(02):317–323, 1983, Online.

[26] R. Cairns. *Radiofrequency heating of plasmas*. A. Hilger, Bristol, England Philadelphia, 1991. ISBN 0750300345.

[27] L.-G. Eriksson, T. Hellsten, M. F. F. Nave, et al. Toroidal rotation in RF heated JET plasmas. *Plasma Physics and Controlled Fusion*, 51(4):044008, 2009, Online.

[28] M. F. F. Nave, T. Johnson, L.-G. Eriksson, et al. Influence of magnetic field ripple on the intrinsic rotation of tokamak plasmas. *Phys. Rev. Lett.*, 105:105005, Sep 2010, Online.

[29] T. Hellsten, T. J. Johnson, D. Van Eester, et al. Observations of rotation in JET plasmas with electron heating by ion cyclotron resonance heating. *Plasma Physics and Controlled Fusion*, 54(7):074007, 2012, Online.

[30] Y. Lin, J. E. Rice, S. J. Wukitch, et al. Observation of ion-cyclotron-frequency mode-conversion flow drive in tokamak plasmas. *Phys. Rev. Lett.*, 101:235002, Dec 2008, Online.

[31] Y. Lin, P. Mantica, T. Hellsten, et al. Ion cyclotron range of frequency mode conversion flow drive in D(^{3}He) plasmas on JET. *Plasma Physics and Controlled Fusion*, 54(7):074001, 2012, Online.

[32] P. N. Yushmanov. *Reviews of plasma physics*, 16:117, 1990.

[33] K. Tani, T. Takizuka, and M. Azumi. Ripple loss of alpha particles in a tokamak reactor with a noncircular plasma cross-section. *Nuclear Fusion*, 33(6):903, 1993, Online.

[34] R. J. Goldston and H. H. Towner. Effects of toroidal field ripple on suprathermal ions in tokamak plasmas. *Journal of Plasma Physics*, 26(02):283–307, 1981, Online.

[35] R. J. Goldston, R. B. White, and A. H. Boozer. Confinement of high-energy trapped particles in tokamaks. *Phys. Rev. Lett.*, 47:647–649, Aug 1981, Online.

[36] K. C. Shaing. Magnetohydrodynamic-activity-induced toroidal momentum dissipation in collisionless regimes in tokamaks. *Physics of Plasmas*, 10(5):1443–1448, 2003, Online.

[37] K. C. Shaing, M. S. Chu, and S. A. Sabbagh. Eulerian approach to bounce/transit and drift resonance and neoclassical toroidal plasma viscosity in tokamaks. *Plasma Physics and Controlled Fusion*, 51(7):075015, 2009, Online.

[38] K. C. Shaing, S. A. Sabbagh, and M. S. Chu. Neoclassical toroidal plasma viscosity in the superbanana plateau regime for tokamaks. *Plasma Physics and Controlled Fusion*, 51(3):035009, 2009, Online.

[39] K. C. Shaing, S. A. Sabbagh, and M. S. Chu. Neoclassical toroidal plasma viscosity in the superbanana regime in tokamaks. *Plasma Physics and Controlled Fusion*, 51(5):055003, 2009, Online.

[40] Y. Sun, Y. Liang, K. C. Shaing, et al. Neoclassical toroidal plasma viscosity torque in collisionless regimes in tokamaks. *Phys. Rev. Lett.*, 105:7145002, Oct 2010, Online.

[41] A. J. Cole, J. D. Callen, W. M. Solomon, et al. Peak neoclassical toroidal viscosity at low toroidal rotation in the DIII-D tokamak. *Physics of Plasmas*, 18(5):055711, 2011, Online.

[42] A. Romannikov, C. Bourdelle, J. Bucalossi, et al. Measurement of central toroidal rotation in ohmic Tore Supra plasmas. *Nuclear Fusion*, 40(3):319–324, Mar 2000, Online.

[43] V. Basiuk, Y. Peysson, M. Lipa, et al. Studies of suprathermal electron loss in the magnetic ripple of Tore Supra. *Nuclear Fusion*, 41(5):477, 2001, Online.

[44] F. L. Hinton and J. A. Robertson. Neoclassical dielectric property of a tokamak plasma. *Physics of Fluids*, 27(5):1243–1247, 1984. doi: 10.1063/1.864478, Online.

[45] R. C. Morris, M. G. Haines, and R. J. Hastie. The neoclassical theory of poloidal flow damping in a tokamak. *Physics of Plasmas*, 3(12):4513–4520, 1996, Online.

[46] C. T. Hsu, K. C. Shaing, and R. Gormley. Time dependent parallel viscosity and relaxation rate of poloidal rotation in the banana regime. *Physics of Plasmas*, 1(1): 132–138, 1994, Online.

[47] S. P. Hirshman. The ambipolarity paradox in toroidal diffusion, revisited. *Nuclear Fusion*, 18(7):917, 1978, Online.

[48] K. C. Shaing and S. P. Hirshman. Relaxation rate of poloidal rotation in the banana regime in tokamaks. *Physics of Fluids B: Plasma Physics*, 1(3):705–707, 1989, Online.

[49] K. Nagashima, Y. Koide, and H. Shirai. Experimental determination of non-diffusive toroidal momentum flux in JT-60U. *Nuclear Fusion*, 34(3):449, 1994, Online.

[50] K. Ida, Y. Miura, T. Matsuda, et al. Evidence for a toroidal-momentum-transport nondiffusive term from the JFT-2M tokamak. *Phys. Rev. Lett.*, 74:1990–1993, Mar 1995, Online.

[51] M. Yoshida, Y. Koide, H. Takenaga, et al. Momentum transport and plasma rotation profile in toroidal direction in JT60-U L-mode plasmas. *Nuclear Fusion*, 47(8):856, 2007, Online.

[52] T. Tala, K.-D. Zastrow, J. Ferreira, et al. Evidence of inward toroidal momentum convection in the JET tokamak. *Phys. Rev. Lett.*, 102:075001, Feb 2009, Online.

[53] W. M. Solomon, K. H. Burrell, A. M. Garofalo, et al. Advances in understanding the generation and evolution of the toroidal rotation profile on DIII-D. *Nuclear Fusion*, 49(8):085005, 2009, Online.

[54] S. M. Kaye, W. Solomon, R. E. Bell, et al. Momentum transport in electron-dominated NSTX spherical torus plasmas. *Nuclear Fusion*, 49(4):045010, 2009, Online.

[55] A. G. Peeters, C. Angioni, and D. Strintzi. Toroidal momentum pinch velocity due to the coriolis drift effect on small scale instabilities in a toroidal plasma. *Phys. Rev. Lett.*, 98:265003, Jun 2007, Online.

[56] A. G. Peeters, C. Angioni, A. Bortolon, et al. Overview of toroidal momentum transport. *Nuclear Fusion*, 51(9):094027, 2011, Online.

[57] T. S. Hahm, P. H. Diamond, O. D. Gurcan, and G. Rewoldt. Nonlinear gyrokinetic theory of toroidal momentum pinch. *Physics of Plasmas*, 14(7):072302, 2007, Online.

[58] P. H. Diamond, C. J. McDevitt, Ö. D. Gürcan, T. S. Hahm, and V. Naulin. Transport of parallel momentum by collisionless drift wave turbulence. *Physics of Plasmas*, 15(1):012303, 2008, Online.

[59] J. S. deGrassie. Tokamak rotation sources, transport and sinks. *Plasma Physics and Controlled Fusion*, 51(12):124047, 2009, Online.

[60] K.-D. Zastrow, W. G. F. Core, L.-G. Eriksson, et al. Transfer rates of toroidal angular momentum during neutral beam injection. *Nuclear Fusion*, 38(2):257, 1998, Online.

[61] S. D. Scott, P. H. Diamond, R. J. Fonck, et al. Local measurements of correlated momentum and heat transport in the TFTR tokamak. *Phys. Rev. Lett.*, 64:531–534, Jan 1990, Online.

[62] J. S. deGrassie, D. R. Baker, K. H. Burrell, et al. Toroidal rotation in neutral beam heated discharges in DIII-D. *Nuclear Fusion*, 43(2):142, 2003, Online.

[63] P.C. de Vries, M.-D. Hua, D.C. McDonald, et al. Scaling of rotation and momentum confinement in JET plasmas. *Nuclear Fusion*, 48(6):065006, 2008, Online.

[64] J. Weiland, A. Eriksson, H. Nordman, and A. Zagorodny. Progress on anomalous transport in tokamaks, drift waves and nonlinear structures. *Plasma Physics and Controlled Fusion*, 49(5A):A45, 2007, Online.

[65] N. Mattor and P. H. Diamond. Momentum and thermal transport in neutral-beam-heated tokamaks. *Physics of Fluids*, 31(5):1180–1189, 1988, Online.

[66] J. E. Rice, A. Ince-Cushman, J. S. deGrassie, et al. Inter-machine comparison of intrinsic toroidal rotation in tokamaks. *Nuclear Fusion*, 47(11):1618, 2007, Online.

[67] P. Mantica, T. Tala, J. S. Ferreira, et al. Perturbative studies of toroidal momentum transport using neutral beam injection modulation in the Joint European Torus: Experimental results, analysis methodology, and first principles modeling. *Physics of Plasmas*, 17(9):092505, 2010, Online.

[68] G. Tardini, A. G. Peeters, G. V. Pereverzev, F. Ryter, and the ASDEX Upgrade Team. Theory-based modelling of ASDEX Upgrade discharges with ECH modulation. *Nuclear Fusion*, 42(7):L11, 2002, Online.

[69] G. Tardini, J. Ferreira, P. Mantica, et al. Angular momentum studies with NBI modulation in JET. *Nuclear Fusion*, 49(8):085010, 2009, Online.

[70] F. Ryter, C. Angioni, C. Giroud, et al. Simultaneous analysis of ion and electron heat transport by power modulation in JET. *Nuclear Fusion*, 51(11):113016, 2011, Online.

[71] F. Ryter, C. Angioni, A. G. Peeters, et al. Experimental study of trapped-electron-mode properties in tokamaks: Threshold and stabilization by collisions. *Phys. Rev. Lett.*, 95:085001, Aug 2005, Online.

[72] F. X. Söldner, K. McCormick, D. Eckhartt, et al. Suppression of sawtooth oscillations by lower-hybrid current drive in the ASDEX tokamak. *Phys. Rev. Lett.*, 57: 1137–1140, Sep 1986, Online.

[73] D. J. Campbell, D. F. H. Start, J. A. Wesson, et al. Stabilization of sawteeth with additional heating in the JET tokamak. *Phys. Rev. Lett.*, 60:2148–2151, May 1988, Online.

[74] C. R. Negus, C. Giroud, A. G. Meigs, et al. Enhanced core charge exchange recombination spectroscopy system on Joint European Torus. *Review of Scientific Instruments*, 77(10):10F102, 2006, Online.

[75] J. A. Heikkinen and S. K. Sipilä. Power transfer and current generation of fast ions with large-k_θ waves in tokamak plasmas. *Physics of Plasmas*, 2(10):3724–3733, 1995, Online.

[76] J. A. Heikkinen, W. Herrmann, and T. K. Kurki-Suonio. Fast response in the ripple trapped ion distribution to abrupt changes in a radial electric field in tokamaks. *Nuclear Fusion*, 38(3):419, 1998, Online.

[77] T. Johnson, A. Salmi, G. Steinbrecher, et al. Library for RF interactions in orbit following codes. *AIP Conference Proceedings*, 1406(1):373–376, 2011, Online.

[78] K. Shinohara, T. Kurki-Suonio, D. Spong, et al. Effects of complex symmetry-breakings on alpha particle power loads on first wall structures and equilibrium in ITER. *Nuclear Fusion*, 51(6):063028, 2011, Online.

[79] T. Kurki-Suonio, O. Asunta, E. Hirvijoki, et al. Fast ion power loads on ITER first wall structures in the presence of NTMs and microturbulence. *Nuclear Fusion*, 51 (8):083041, 2011, Online.

[80] M. García-Muñoz, P. Martin, H.-U. Fahrbach, et al. NTM induced fast ion losses in ASDEX Upgrade. *Nuclear Fusion*, 47(7):L10, 2007, Online.

[81] G. Park, C. S. Chang, I. Joseph, and R. A. Moyer. Plasma transport in stochastic magnetic field caused by vacuum resonant magnetic perturbations at diverted tokamak edge. *Physics of Plasmas*, 17(10):102503, 2010, Online.

[82] Y. Sun, Y. Liang, H. R. Koslowski, et al. Toroidal rotation braking with n = 1 magnetic perturbation field on JET. *Plasma Physics and Controlled Fusion*, 52 (10):105007, 2010, Online.

[83] Y. Liang, H. R. Koslowski, P. R. Thomas, et al. Active control of type-I edge-localized modes with $n = 1$ perturbation fields in the JET tokamak. *Phys. Rev. Lett.*, 98: 265004, Jun 2007, Online.

[84] S. K. Sipilä. *ASCOT: accelerated simulation of charged particle orbits in a Tokamak*. TKK, PhD Thesis, Espoo, 1992. ISBN 951-22-1137-8.

[85] V. Hynönen. *Orbit-following simulation of fast ions in ASDEX upgrade tokamak in the presence of magnetic ripple and radial electric field*. Helsinki University of Technology, PhD Thesis, Espoo, 2008. ISBN 978-951-22-9459-6, Online.

[86] G. Genacchi and A. Taroni. JETTO: a free boundary plasma transport code (basic version). *Rapporto ENEA RT/TIB*, 1988.

[87] L. L. Lao, J. R. Ferron, R. J. Groebner, et al. Equilibrium analysis of current profiles in tokamaks. *Nuclear Fusion*, 30(6):1035, 1990, Online.

[88] L.-G. Eriksson and M. Schneider. Monte Carlo operators for ions interacting with radio frequency waves. *Physics of Plasmas*, 12(7):072524, 2005, Online.

[89] P. Strand, I. C. Plasencia, B. Guillerminet, et al. A european infrastructure for fusion simulations. In *Parallel, Distributed and Network-Based Processing (PDP), 2010 18th Euromicro International Conference on*, pages 460–467, Feb 2010, Online.

[90] L.-G. Eriksson, T. Hellsten, and U. Willen. Comparison of time dependent simulations with experiments in ion cyclotron heated plasmas. *Nuclear Fusion*, 33(7): 1037, 1993, Online.

[91] L.-G. Eriksson and T. Hellsten. A model for calculating ICRH power deposition and velocity distribution. *Physica Scripta*, 52(1):70, 1995, Online.

[92] J. Carlsson, L.-G. Eriksson, and T. Hellsten. FIDO, a code for calculating the velocity distribution function of a toroidal plasma during ICRH. In *Theory of Fusion Plasmas*, page 351, Varenna, 1994. Joint Varenna-Lausanne International Workshop, Societá Italiana di Fisica.

[93] L.-G. Eriksson, M. J. Mantsinen, V. P. Bhatnagar, et al. Theoretical analysis of ICRF heating in JET DT plasmas. *Nuclear Fusion*, 39(3):337, 1999, Online.

[94] M. J. Mantsinen, O. N. Jarvis, V. G. Kiptily, et al. First observation of pT fusion in JET tritium plasmas with ICRF heating of protons. *Nuclear Fusion*, 41(12):1815, 2001, Online.

[95] L.-G. Eriksson and P. Helander. Monte Carlo operators for orbit-averaged Fokker–Planck equations. *Physics of Plasmas*, 1(2):308–314, 1994, Online.

[96] L.-G. Eriksson, M. J. Mantsinen, T. Hellsten, and J. Carlsson. On the orbit-averaged Monte Carlo operator describing ion cyclotron resonance frequency wave–particle interaction in a tokamak. *Physics of Plasmas*, 6(2):513–518, 1999, Online.

[97] A. A. Korotkov, A. Gondhalekar, and A. J. Stuart. Impurity induced neutralization of megaelectronvolt energy protons in JET plasmas. *Nuclear Fusion*, 37(1):35, 1997, Online.

[98] L.-G. Eriksson, M. J. Mantsinen, F. G. Rimini, et al. ICRF heating of JET plasmas with the third harmonic deuterium resonance. *Nuclear Fusion*, 38(2):265, 1998, Online.

[99] C. D. Challis, J. G. Cordey, H. Hamnén, et al. Non-inductively driven currents in JET. *Nuclear Fusion*, 29(4):563, 1989, Online.

[100] G. Saibene, R. Sartori, P. de Vries, et al. Toroidal field ripple effects on H-modes in JET and implications for ITER. *Proc. 34th EPS Conf. on Plasma Physics Controlled Fusion (Warsaw, Poland, 2007)*, Online.

[101] K. Tobita, K. Tani, Y. Neyatani, et al. Ripple-trapped loss of neutral-beam-injected fast ions in JT-60U. *Phys. Rev. Lett.*, 69:3060–3063, Nov 1992, Online.

[102] T. Johnson, J. Lönnroth, P.C. de Vries, et al. HALEKAR modelling of fast particle transport and losses with TF ripple in JET. In *10th IAEA Technical Meeting on Energetic Particles in Magnetic Confinement Systems*.

[103] H. Biglari, P. H. Diamond, and P. W. Terry. Influence of sheared poloidal rotation on edge turbulence. *Physics of Fluids B: Plasma Physics*, 2(1):1–4, 1990, Online.

[104] R. J. Goldston, D. C. McCune, H. H. Towner, et al. New techniques for calculating heat and particle source rates due to neutral beam injection in axisymmetric tokamaks. *Journal of Computational Physics*, 43(1):61–78, 1981, Online.

[105] A.G. Peeters, Y. Camenen, F.J. Casson, et al. The nonlinear gyro-kinetic flux tube code GKW. *Computer Physics Communications*, 180(12):2650 – 2672, 2009. ISSN 0010-4655, Online.

[106] M. A. Kotschenreuther, G. B. Rewoldt, and W. M. B. Tang. Comparison of initial value and eigenvalue codes for kinetic toroidal plasma instabilities. *Computer Physics Communications*, 88(2-3):128–140, 1995, Online.

[107] A. G. Peeters, C. Angioni, A. Bottino, et al. Toroidal momentum transport. *Plasma Physics and Controlled Fusion*, 48(12B):B413, 2006, Online.

[108] J. E. Kinsey, R. E. Waltz, and J. Candy. Nonlinear gyrokinetic turbulence simulations of E x B shear quenching of transport. *Physics of Plasmas*, 12(6):062302, 2005, Online.

[109] D. Strintzi, A. G. Peeters, and J. Weiland. The toroidal momentum diffusivity in a tokamak plasma: A comparison of fluid and kinetic calculations. *Physics of Plasmas*, 15(4):044502, 2008, Online.

[110] A. G. Peeters, C. Angioni, and ASDEX Upgrade Team. Linear gyrokinetic calculations of toroidal momentum transport in a tokamak due to the ion temperature gradient mode. *Physics of Plasmas*, 12(7):072515, 2005, Online.

[111] R. J. Hawryluk, D. J. Campbell, G. Janeschitz, et al. Principal physics developments evaluated in the ITER design review. *Nuclear Fusion*, 49(6):065012, 2009, Online.

[112] A. Portone, M. Roccella, R. Roccella, F. Lucca, and G. Ramogida. The ITER TF coil ripple: Evaluation of ripple attenuation using Fe insert and of ripple enhancement produced by TBM. *Fusion Engineering and Design*, 83(10-12):1619–1624, 2008. ISSN 0920-3796, Online. Proceedings of the Eight International Symposium of Fusion Nuclear Technology, ISFNT-8 SI.

[113] H. Kawashima, M. Sato, K. Tsuzuki, et al. Demonstration of ripple reduction by ferritic steel board insertion in JFT-2M. *Nuclear Fusion*, 41(3):257, 2001, Online.

[114] K. Shinohara, H. Kawashima, K. Tsuzuki, et al. Effects of complex magnetic ripple on fast ions in JFT-2M ferritic insert experiments. *Nuclear Fusion*, 43(7):586, 2003, Online.

[115] K. Shinohara, S. Sakurai, M. Ishikawa, et al. Ferritic insertion for reduction of toroidal magnetic field ripple on JT-60U. *Nuclear Fusion*, 47(8):997, 2007, Online.

VTT Publications
VTT Science 10

Title	**Fast ions and momentum transport in JET tokamak plasmas**
Author	Antti Salmi
Abstract	Fast ions are an inseparable part of fusion plasmas. They can be generated using electromagnetic waves or injected into plasmas as neutrals to heat the bulk plasma and to drive toroidal rotation and current. In future power plants fusion born fast ions deliver the main heating into the plasma. Understanding and controlling the fast ions is of crucial importance for the operation of a power plant. Furthermore, fast ions provide ways to probe the properties of the thermal plasma and get insight of its confinement properties. In this thesis, numerical code packages are used and developed to simulate JET experiments for a range of physics issues related to fast ions. Namely, the clamping fast ion distribution at high energies with RF heating, fast ion ripple torque generation and the toroidal momentum transport properties using NBI modulation technique are investigated. Through a comparison of numerical simulations and the JET experimental data it is shown that the finite Larmor radius effects in ion cyclotron resonance heating are important and that they can prevent fast ion tail formation beyond certain energy. The identified mechanism could be used for tailoring the fast ion distribution in future experiments. Secondly, ASCOT simulations of NBI ions in a ripple field showed that most of the reduction of the toroidal rotation that has been observed in the JET enhanced ripple experiments could be attributed to fast ion ripple torque. Finally, fast ion torque calculations together with momentum transport analysis have led to the conclusion that momentum transport in not purely diffusive but that a convective component, which increases monotonically in radius, exists in a wide range of JET plasmas. Using parameter scans, the convective transport has been shown to be insensitive to collisionality and q-profile but to increase strongly against density gradient.
ISBN, ISSN	ISBN 978-951-38-7467-4 (soft back edition) ISSN 2242-119X (soft back edition) ISBN 978-951-38-7468-1 (http://www.vtt.fi/publications/index.jsp) ISSN 2242-1203 (http://www.vtt.fi/publications/index.jsp)
Date	October 2012
Language	English, Finnish abstract
Pages	71 p. + app 75 p.
Keywords	JET, tokamak, fusion, energy, plasma, toroidal rotation, momentum transport, fast ions, neutral beam injection, NBI
Publisher	VTT Technical Research Centre of Finland P.O. Box 1000, FI-02044 VTT, Finland, Tel. 020 722 111

VTT Publications
VTT Science 10

Nimike	**Nopeat ionit ja liikemäärän kulkeutuminen JET-tokamakin plasmoissa**
Tekijä	Antti Salmi
Tiivistelmä	Nopeat ionit ovat erottamaton osa fuusioplasmoja. Niitä voidaan tuottaa sähkömagneettisten aaltojen avulla tai suihkuttamalla ne plasmaan energisinä neutraaleina. Nopeita ioneja käytetään kuumentamaan ja pyörittämään plasmaa, virranajossa sekä plasman ominaisuuksien ja koossapidon tutkimiseen. Tulevaisuuden voimalaitoksissa fuusioreaktioissa syntyvät nopeat ionit toimivat plasman pääasiallisena lämmönlähteenä. Nopeiden ionien ilmiöiden ymmärtäminen ja niiden hallinta ovat tärkeitä fuusiovoimaloiden operoinnin kannalta. Tässä väitöstyössä käytetään ja kehitetään numeerisia laskentaohjelmia selittämään nopeisiin ioneihin liittyviä koetuloksia Englannissa sijaitsevassa fuusiokoelaitoksessa (JET). Tutkimuksen kohteina ovat nopeiden ionien äkillinen väheneminen korkeilla energioilla radiotaajuuskuumennuksen yhteydessä, nopeiden ionien aiheuttama toroidaalinen vääntö magneettikentän ryppyisyyden vaikutuksesta ja liikemäärän kulkeutumisen ominaisuudet moduloituja neutraalisuihkuja käyttäen. Työssä todennettiin simuloinneilla, että ionien äärellinen pyörimissäde selittää kokeellisesti havaitun nopeiden ionien pienen lukumäärän korkeilla energioilla käytettäessä radiotaajuuskuumennusta. JET:n magneettikentän rypytyskokeissa havaitut plasman pyörimisen muutokset voitiin hiukkassimulointien avulla päätellä johtuvan pääasiassa nopeiden ionien synnyttämän väännön takia. Lopulta analyysit liikemäärän kulkeutumisesta useissa erilaisissa plasmoissa osoittivat, että liikemäärän kulkeutuminen ei ole pelkästään diffuusia ja että merkittäväksi osoittautunut koossapitoa parantava ajautumisnopeus kasvaa plasman ulkoreunaa lähestyttäessä. Plasman tiheysgradientin kasvattamisen havaittiin nopeasti kasvattavan ajautumisnopeutta, kun taas törmäyksellisyyden tai q-profiilin muutosten vaikutukset olivat pieniä. Työn tuloksia voidaan hyödyntää ITERin ja tulevien laitosten suunnittelussa ja plasman pyörimisen ennustuksissa.
ISBN, ISSN	ISBN 978-951-38-7467-4 (nid.) ISSN 2242-119X (nid.) ISBN 978-951-38-7468-1 (http://www.vtt.fi/publications/index.jsp) ISSN 2242-1203 (http://www.vtt.fi/publications/index.jsp)
Julkaisuaika	Lokakuu 2012
Kieli	Englanti, suomenkielinen tiivistelmä
Sivumäärä	71 s. + liit. 75 s.
Avainsanat	JET, tokamak, fusion, energy, plasma, toroidal rotation, momentum transport, fast ions, neutral beam injection, NBI
Julkaisija	VTT Technical Research Centre of Finland PL 1000, FI-02044 VTT, Finland, Puh. 020 722 111

Fast ions and momentum transport in JET tokamak plasmas

Energy production and consumption are strongly linked with critical environmental issues such as global warming. Today more than 80 % of our primary energy is obtained by burning fossil fuels. It is widely recognised that cleaner and more sustainable forms of energy are needed. Nuclear fusion between heavy hydrogen isotopes has the potential to provide an abundant and environmentally friendly form of energy for the future.

Currently, the most advanced concept for a fusion power plant is a tokamak. Inside its torus shaped chamber, the fuel, in a form of plasma, must be confined and heated to over 100 million degrees and kept clear from the surrounding walls to initiate the fusion reactions. The economic viability of fusion power is largely determined by the degree of plasma confinement that can be achieved. Experiments have shown that by spinning the plasma in toroidal direction its confinement is improved and that certain instabilities can be mitigated thus improving the fusion performance.

Fast ions are responsible for most of the plasma rotation in present day tokamaks. This research is focused on fast ions as a rotation source and as a tool for studying the toroidal rotation and momentum transport properties of the JET tokamak plasmas. Numerical code packages are developed and validated against the experimental data paving the way for predictive modelling capabilities.

ISBN 978-951-38-7467-4 (soft back ed.)
ISBN 978-951-38-7468-1 (URL: http://www.vtt.fi/publications/index.jsp)
ISSN 2242-119X (soft back ed.)
ISSN 2242-1203 (URL: http://www.vtt.fi/publications/index.jsp)